FACULDADE DE ENGENHARIA DA UNIVERSIDADE DO PORTO

Reconfigurable acoustic modem for underwater communications

Luis Ungaro Pinto Coelho

FOR JURY EVALUATION

Mestrado Integrado em Engenharia Eletrotécnica e de Computadores

Supervisor: Prof. José Carlos Alves

June 29, 2015

Resumo

As comunicações acústicas subaquáticas têm suscitado um interesse crescente na comunidade científica ao longo das últimas décadas. Tal interesse é justificado não só pela grande variedade de aplicações que beneficiam deste tipo de comunicações, mas também pelo considerável desenvolvimento que se tem verificado nesta área. De facto, existem atualmente muitas soluções interessantes tanto a nível académico como comercial. Contudo, a reduzida flexibilidade dos parâmetros inerentes ao funcionamento de tais dispositivos torna-os pouco adaptáveis à grande variabilidade de condições que se verifica no meio subaquático. Por outro lado, as soluções existentes são pouco escaláveis e não é viável utilizar as mesmas como base para desenvolvimentos posteriores.

Esta dissertação diz respeito ao desenvolvimento de um modem acústico subaquático reconfigurável com modulação FSK que dispõe da desejada flexibilidade pelo que pode ser ajustado mediante o meio em que se encontra, podendo também ser utilizado para desenvolvimento e teste de novos projetos. Mais concretamente, o trabalho aqui apresentado fará uso de um modem FSK já desenvolvido, tendo como objetivo a seleção e implementação de estratégias que permitam a melhoria do seu desempenho.

Abstract

The field of underwater acoustic communications has received an increasing attention over the last decades. This is due to the wide variety of applications that rely on such form of communication and also to the great developments this field is constantly undertaking. In fact, there are currently several interesting solutions of both academic and commercial nature. However, the reduced flexibility of the parameters regarding these systems' operation is not suited to the high variability of in loco conditions in underwater channels. Furthermore, these solutions were not designed with scalability in mind, and thus they do not provide a basic structure upon which further developments can be made.

This dissertation regards the development of a reconfigurable underwater acoustic modem based upon FSK modulation. This platform allows for the desired flexibility as it can be easily readjusted and can also be used as a reference project for the development and testing of new designs. More specifically, the work presented herein will regard a previously developed FSK modem, aiming for increasing its performance through a careful selection and implementation of new features.

Agradecimentos

Não poderia deixar de expressar o meu profundo agradecimento ao Professor José Carlos Alves, não só por me ter proposto este desafio, mas sobretudo pelo acompanhamento incansável tanto a nível académico como a nível pessoal ao longo desta dissertação. Devo referir, ainda, o impacto que o seu entusiasmo inabalável teve nos momentos em que tudo parecia perdido e o facto de tão prontamente ter disponibilizado, além de tempo, os seus próprios recursos em prol desta dissertação.

Gostaria também de agradecer ao Henrique Cabral, autor do trabalho a que esta dissertação dá continuidade, por se ter mostrado sempre disponível para esclarecer as dúvidas que foram surgindo.

Luis Ungaro

"As Gregor Samsa awoke one morning from uneasy dreams
he found himself transformed in his bed into a gigantic insect"

Franz Kafka

Contents

List of Figures

Abbreviations

BFSK	Binary Frequency-Shift Keying
DFE	Decision Feedback Equalizer
DPSK	Differential Phase-Shift Keying
DSB	Double-Sideband
FFT	Fast Fourier Transform
FIR	Finite Impulse Response
FPGA	Field-Programmable Gate Array
FSK	Frequency-Shift Keying
IIR	Infinite Impulse Response
ISI	Intersymbol Interference
LMS	Least Mean Squares
MCM	Multi-Carrier Modulations
MFSK	Multiple Frequency-Shift Keying
MIMO	Multiple-Input and Multiple-Output
ML	Maximum Likelihood
MLSE	Maximum Likelihood Sequence Estimation
MSE	Mean Squared Error
MT-FSK	Multiple Tone Frequency-Shift Keying
OFDM	Orthogonal Frequency-Division Multiplexing
PLL	Phase-Locked Loop
PSK	Phase-Shift Keying
RLS	Recursive Least Squares
SNR	Signal-to-Noise Ratio

Chapter 1

Introduction

The need for underwater wireless communications arises from several applications, such as the energy industry, the scientific study of the oceanic environment, the communication between vehicles, the recognition of the surrounding space and even more commercially oriented applications. Among these, the nature of the transmitted signals can be divided into control, telemetry, speech and video, in an ordering of increasing data rates. Although these applications have not changed much in recent years (besides the increase of commercial applications), their demands have grown continuously.

Since electromagnetic waves are widely used in many applications, they could be thought of as the natural choice to perform such communication. However, in the underwater channel, these suffer from scattering and also from the medium's conductivity. The first effect creates the requirement of narrow laser beams and the second makes the propagation range acceptable only for very low frequencies. For these reasons, acoustic waves are the most appropriate form of underwater communication, even if they still suffer from a fair share of adverse effects.

Naturally, researches attempted to transpose many important principals of wireless communications, mutatis mutandis, to their underwater acoustic counterparts. In fact, important analogies can be made, however, the particular nature of the channel, along with the associated undesirable properties, requires more specialized communication techniques. Consequently, throughout the years, a plethora of systems and techniques has been developed for this purpose, as well as channel models to support them. Nevertheless, "Just as in telemetry over electromagnetic channels, there is no single design of an acoustic telemetry system appropriate for all environments" [2]. In fact, as the variability of in loco conditions precludes an universal characterization of underwater acoustic channels, each approach is either focused only on a specific set of channels or is not exactly optimized for any usage scenario. Furthermore, both academic and commercial solutions are usually not designed with extensibility in mind neither do they allow for simple structural modifications. Therefore, nearly all the mentioned applications would benefit from the existence of a re-configurable and extensible platform, as it would allow for a straightforward parameter optimization and would also serve as a framework for further developments.

This dissertation consists of the development of such platform in the form of an underwater

acoustic modem. More specifically, it is intended to study the work presented in [3], wherein a complete FSK modem was developed, and to enhance this fundamental structure by increasing its robustness and data rates. To that end, the state of the art will be presented in section 2 so as to provide an insight on the key aspects of underwater acoustic communications (which is by itself an extensive topic), followed by presentation of the corresponding solutions and systems developed throughout the years. In Ch. 3, a brief description of the previously developed system is presented, while a preliminary set of experiments with the goal of better understanding the most critical aspects of its performance is presented in Ch. 4. A careful selection of the features to be implemented as well as their actual implementation details are presented in Ch. 5. Finally, the results of such modifications are presented in Ch. 6 followed by the conclusions that could be derived from this dissertation in Ch. 7.

Chapter 2

State of the art

2.1 Introduction

Although the idea of conveying information underwater through the use of sound is hundreds of old, modern underwater acoustic communications arose in the second half of the XX century.

Specifically, the first systems were designed in the seventies, and were based upon the robust non-coherent modulations, mainly FSK, since coherent detection was still a complex issue due to the harsh characteristics of the underwater acoustic channel. Digital systems allowed for the use of techniques such as error correction as well as time and frequency dispersion compensation, however, since that time, there was not a major development of systems based upon incoherent modulation, mainly because of their spectral inefficient nature.

The efficiency of coherent detection-based systems, that could make them capable of providing high data rate communications, made researchers analyze more thoroughly the feasibility of this kind of modulation. In fact, in the 90's, the development of coherent-based communication systems emerged, with several successful implementations, even in shallow water horizontal channels. Consequently, the associated increase in the effective data rate broadened the horizon of underwater communications.

The design of such systems, once thought to be unfeasible, was only possible because of the use of signal processing techniques relying on faithful channel modeling. In fact, this is one of the key issues of underwater acoustic communications, since it was the study of the properties of the channel that drove the course of this field from the beginning. The knowledge of the channel's properties, along with all the important conclusions that it allowed to be drawn, was responsible not only for the use of the modulation schemes that were more appropriate for the matter, but also for more complex and reliable receiver designs.

Of course, such complex systems, would not have been designed without the exponential growth of cheap processing power. Thanks to it, and the resulting availability of powerful off-the-shelf components, such as microprocessors and FPGA's, the development of an underwater acoustic system today is hardly conditioned by hardware limitations. Additionally, they allow for more flexible systems and increased scalability, since they can be easily reprogrammed.

The new century brought even more complex designs into the underwater channel, as several papers describe the use of multi-carrier modulations (MCM) as well as MIMO techniques. In parallel with all this developments, networking in the underwater channel has also drawn an increasing attention.

2.2 The underwater acoustic channel

The underwater acoustic channel is a harsh medium for the establishment wireless communications. This is due to signal independent factors, such as noise, and also to several modifications that sound undertakes while it propagates. Therefore, it is of extreme importance to gain insight, in the first place, on such characteristics of the channel, and afterwards to use such piece of information to understand the corresponding consequences to the course of communication. It is important to point out that, as stated above, there is no universally accepted characterization of the underwater acoustic channel. As such, the purpose of the following discussion is to provide an generic and essential background that should allow for a coherent approach to problem.

2.2.1 Underwater sound

Attenuation

In the underwater acoustic channel there are two main causes of sound attenuation. The first, is the spreading loss, which is due to the unfocused nature of sound and consists of its energy being spread on a continuously larger surface centered in the point of emission. Of course, if the surface enlarges, the energy at a given point of the surface gets smaller. Thus, the impact of this frequency independent phenomenon increases with the distance between transmitter and receiver.

The second cause of attenuation is absorption, which consists of the dissipation of the acoustic wave energy, i.e. its conversion into heat. The amount of attenuation introduced by this effect, while still dependent on the distance, depends also on the frequency of the signal. More specifically, it increases with the frequency, and as it will be seen further, this has important consequences.

Taking into account these effects, [4] states that the overall attenuation (or path loss) is given by

$$A(l,f) = (l/l_r)^k a(f)^{l_r - l} \tag{2.1}$$

where l is the transmission distance in reference to l_r, f is the signal frequency, $a(f)$ is the absorption coefficient and k models the spreading loss. It is important to mention that $a(f)$ increases with frequency and thus, the overall attenuation follows this behavior.

Noise

Regarding the noise, it also plays an important role in the underwater acoustic communication. While its presence is more prominent near the surface, it can arise from several sources [5], many

of these being site- and frequency-dependent, and each producing noise of its own nature. Ambient noise, can be modeled by a continuous spectrum and a Gaussian distribution. Despite being Gaussian, ambient noise its not white, in fact, its power spectrum decays at approximately 18db/dec, and has it will be shown further, this has important consequences.

Speed of sound and sound refraction

In fluids, the speed of sound depends mainly on the density and the compressibility. Since in the ocean, the former is related to static pressure, temperature and salinity, sound speed in this medium is a function of this three quantities. Of course, these have generic values in many sites, depending only on the depth. With this in mind, the generic profiles of the relation between sound speed and depth are presented in [6]. Herein, it is shown that in the thermocline layer, a region located at around 1000 feet of depth, the speed of sound has a strong variation, due to the abrupt decrease of temperature. This variation of speed causes sound refraction, and as it will be shown further, this will have important implications in the course of communication.

In any case, the mentioned variations are irrelevant with respect to the relationship between the speed of sound on water and that of the electromagnetic waves on any medium. In fact, the latter is always several orders of magnitude larger then the former, and this will be the cause of another undesirable effect.

Sound reflection and scattering

As it is exposed in [6], the underwater channel acts as a wave guide in regards to the propagation of acoustic signals, and besides the mentioned refraction, it also causes sound reflection. The main causes of reflection are the bottom and surface of the ocean. The former is considered to be a nearly perfect reflector (with a reflection coefficient equal to -1), whereas the latter provides a more complex reflection (depending on the type of bottom surface), with potential loss of energy.

However, these are not the only causes of reflection since it can be caused by any object that might be along the path of the wave, and the nature of the reflection is deeply related to that object's characteristics. In fact, when the surface of incidence is irregular, the wave front is divided into smaller ones, which are reflected in many different directions. This phenomenon is called scattering, and not only it weakens the wave that actually continues to propagate in the right path, but it also causes interference due to the creation of several wave fronts. Nevertheless, for the frequencies of interest in underwater communications this effect can be neglected[5].

2.2.2 Implications borne on the physical layer

With the mentioned properties of the channel in mind, it is possible to conclude on the implications that these have on the course of the communication. In the design of a communication system for the underwater acoustic channel, these are the aspects one is, in fact, ought to consider. Therefore, a correct and clear organization of such implications is now presented.

SNR and bandwidth

The SNR and the available bandwidth are relevant measures to consider in order to understand the capacity of the medium, and in this case, these are deeply related.

As pointed out in [4], the SNR can be described as follows

$$SNR(l,f) = \frac{S_l(f)}{A(l,f)N(f)} \tag{2.2}$$

where, once again, l and f are the transmission distance and the signal's frequency, respectively. $S_l(f)$ is the power spectral density of the transmitted signal, and $A(l,f)$ and $N(f)$ are, respectively, the attenuation and the noise functions mentioned in the previous section. From what has been exposed so far, this equation will probably seem obvious.

From this equation, an interesting conclusion can be drawn. In fact, for a fixed uniform power spectral density of the transmitted signal, say, 1W, and for a given transmission distance, there is always a frequency of transmission that maximizes the SNR. Figure 2.1 shows the SNR as a function of frequency for several transmission distances, with a common set of parameters of the $A(l,f)$ and $N(f)$ (noise) functions.

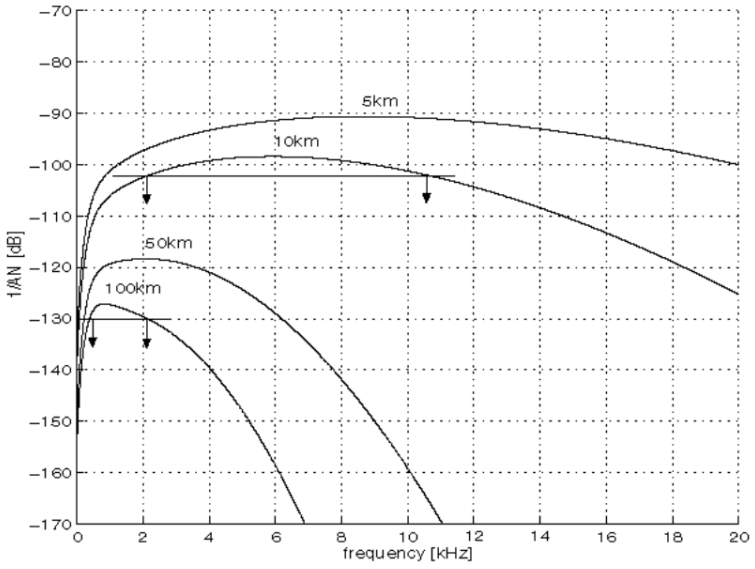

Figure 2.1: SNR with a fixed power spectral density of the transmitted signal, for several transmission distances. The distance between the arrows corresponds to the available bandwidth [4, p. 2].

From this figure and the associated SNR function, there is another important conclusion to be drawn. The available bandwidth with respect to the SNR, i.e. the frequency interval in which the SNR is at the most 3dB shorter then its maximum, also depends on the transmission distance.

Thus, it can be seen that, as expected from the attenuation and noise functions, as the transmission distance increases, the available bandwidth decreases, there is an overall SNR reduction, and the frequency that maximizes it becomes lower. The knowledge of this relationship is important

when conceiving a system the should be able to perform in very different situations, as is the case of this dissertation.

Finally, it is important to point out that among the presented transmission distances, the center frequency is often on the order of the available bandwidth. This observation precludes the use of the narrowband assumption, as the wideband nature of the signal must be considered if all the available bandwidth is used.

Time varying multipath and path dispersion

As mentioned in the previous section, the underwater channel acts as a wave-guide in respect to the transmission of acoustic waves, since the signal reflects and refracts several times along its path, following the ray propagation model[1]. This phenomenon, combined with scattering and the unfocused nature of sound, is responsible for the occurrence of multipath - the arrival of several signal echoes at the receiver, each from a different path. Since each possible path has its own propagation delay and attenuation factor, the received signals will have different phases and amplitudes, respectively. The number of paths is theoretically infinite, but signals echoes that have lost most of their energy can be neglected, thus, only a finite number of paths needs to be considered which essentially depends on the channel's geometry. Of course, this results in signal dispersion in time, considering all the relevant echoes that arrive at the receiver, of an amount on the order of the longest path delay.

On the other hand, the low pass nature of the channel (exposed in its attenuation equation), contributes to the time spreading of individual echoes - an effect termed path dispersion - which will also contribute to time dispersion. An example of the impulse and frequency responses of individual paths and the overall channel are shown in figure 2.2, where it is clear that the most prominent effect is the multipath spread since it is much higher than the path dispersion. The total spread due to both effects is called coherence time of the channel.

Since its impulse response consists of a set of considerably separated discrete multipath arrivals, the underwater channel is considered a sparse multipath channel [4]. This fact enables the use of sparse equalization techniques, as explained below.

It is also important to note that the multipath dispersion is time varying, mainly due to the wave's motion and other inherent changes in the medium. This means that multipath's nature, namely, the number of echoes and the echoes themselves, change over time.

In regards to the transmitter-receiver communication, this effect will result in ISI, due to the mentioned time dispersion, and also in frequency selective fading, since signal echoes with different phases may cause destructive interference. Therefore, from the multipath point of view, the underwater acoustic channel is essentially a fading multipath channel, which is a rather well studied communication medium [7, 8].

Naturally, due to sea surface reflections, the total multipath spread reaches its highest prominence in channels consisting of long horizontal links in shallow water environments.

[1] Although this is not valid for all frequencies, those of interest for underwater acoustic communication justify such approximation [5, 6].

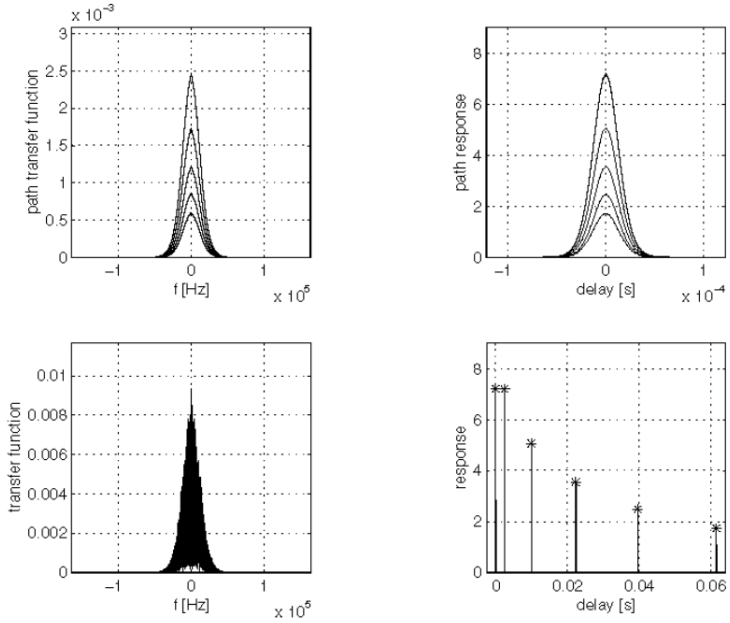

Figure 2.2: Impulse response and transfer functions of individual paths and the overall channel. [4, p. 2]

Doppler Effect

The Doppler effect consists of the different delays that same signal undertakes throughout its extension and it is mainly due to relative motion between the transmitter and the receiver[2], thus, this effect is often noticeable in underwater acoustic channels. This means, for instance, that the signal's leading edge experiences a delay different from that of the signal's trailing edge which results in an overall dilation or compression. Consequently, there is also a dilation or compression in the frequency domain, or, in other words, a frequency shift that depends on the frequency itself[3]. More specifically, each frequency f is shifted by af where a is the ratio between the transmitter-receiver relative speed and the speed of sound - the Doppler factor.

In order to properly model this effect, one must consider the signal as a whole, accounting for all its frequency components, and from that kind of premise it can be shown that the signal faces two forms of distortion. The first is the Doppler shift, which consists of the signal's power spectrum being shifted by af_c, where f_c is its central frequency. The second is the Doppler spread, which presents itself as a global scaling of the signal's bandwidth B by the factor of $(1+a)$, and the corresponding time scaling of the signal by the inverse factor. Therefore, this effect causes a frequency dispersion of the signal. Whereas in narrow-band systems the Doppler spread can be neglected as the shift is almost equal to all frequency components, in wideband systems it must be accounted for. Like multipath, the motion-induced Doppler effect is also time variable, as the

[2]The Doppler Effect can also be caused by channel inherent factors, such as wave drifting, currents and tides. In general, the Doppler effect is due to time variations of the channel which cause changes in the paths' lengths [8, 9]. Herein, the presented analysis focuses on the Doppler effect caused by transmitter-receiver motion.

[3]The fact that the frequency shift increases with frequency is, indeed, an intuitive notion since the amount of motion that originated the Doppler effect corresponds to more wavelengths in higher frequencies

motion between the transmitter and the receiver is hardly constant over a significant amount of time.

2.2.3 Final Considerations

As it can be seen, the underwater acoustic medium imposes many challenges to the establishment of reliable communication.

The frequency-dependent SNR and bandwidth imposes a careful frequency selection for each implementation scenario, and could be further exploited by the use of an automatic frequency selection in response to changes in the channel's characteristics (for that purpose, a feedback channel would obviously be required). Anyway, a distinction of communication channels can be made as to weather these are power or bandwidth limited [8]. Due to the frequency response of the absorption 2.2.1 and the underwater acoustic channel is clearly an example of the latter. As such, an efficient use of the spectrum is required, if high bit rates are to be achieved.

Time varying multipath and Doppler effect combine to create a time and frequency dispersive medium. Despite being, in its essence, a fading multipath channel, the underwater acoustic medium has several distinct characteristics (which must be accounted for). One of these is the path dispersion, i.e. the fact that the path gain decreases with frequency. Another important characteristic is the fact the the Doppler effect is motion induced, rather than simply a consequence of the time variability of the channel. Furthermore, the total multipath spread, can be much larger than that of common radio channels.

The knowledge of these factors, i.e. time spreading (due to multipath) and frequency spreading (due to Doppler, or equivalently time variations of the channel), allows for the estimation of two fundamental measures of the channel[4].

The auto-correlation function of the channel's impulse response at a fixed instant (i.e. considering the channel's impulse response without its time variability) provides the average power output as a function of the path delay. As such, the range of path delays for which this function takes non-null values, say Tm, is the total multipath spread. As explained in [8], the Fourier transform of such function measures the correlation between frequencies as a function of their difference. Naturally, this function will take non-null values in a range equal to $1/Tm$. Therefore an important conclusion can be drawn: if a channel has a multipath spread of Tm seconds, only frequencies separated by more than $1/Tm$ will be affected differently by the channel, and thus $1/Tm$ is termed coherence bandwidth of the channel.

Additionally, there is an underlying trade-off [9] that must be pointed out: increasing the symbol time in order to confine ISI to a smaller number of symbols (as it is done in most multipath fading channels) implies a higher exposure to the time-variability of the channel (as its time-coherence might be exceeded).

A communication system specifically designed for the underwater acoustic channel is required, since common communication schemes would not be able to cope with such harsh effects.

[4] Extended analysis in [8], following the pioneer work first presented by Price.

Of course, it would benefit considerably from signal processing techniques for estimating and removing them.

2.3 Common strategies

Channel modeling guided the communication systems' design as several techniques have been proposed throughout the years as a means of overcoming the undesirable properties of the channel. Some of these explicitly mitigate such issues whereas others simply avoid them. Nevertheless, they can be divided into those based upon the selection of the modulation scheme and those based on careful design of the system's structure, i.e. on the use of individual techniques often independent of the chosen modulation scheme. Techniques regarding both approaches will now be presented, along with the corresponding outcomes in the communication.

2.3.1 Techniques for multipath and Doppler avoidance

Guard intervals

Guard intervals are a simple method to avoid ISI, which consists of inserting delays between successive symbols in order to allow the time reverberation to vanish before the next symbol is transmitted. In other words, the delay aims to exceed the coherence time of the channel. Obviously, this technique results also in a reduction of the data throughput. Examples of the use of this technique can be found in [10].

Frequency hopping

In order to avoid the throughput reduction of guard times, frequency hopping can be employed, i.e. instead of remaining idle during the guard times, the system can transmit on another frequency band. This allows for a more efficient use of the available signal space [2]. Naturally, a frequency separation that exceeds the Doppler spread is mandatory. Examples of the use of this technique can be found in [11, 12].

Diversity Techniques

In fading multipath channels, diversity is based on the notion that errors will occur when the attenuation that the signal is undertaking is large (when the channel is fading). It consists of the transmission of the same signal through different channels, with independent fading, since the probability of simultaneous fading above a critical threshold on all channels is much smaller than on a single one.

In underwater acoustic communications, the most common way of employing this is through the use of different frequency channels separated by guard bands (frequency diversity)[5], i.e. by

[5]This can be considered a special case of frequency hopping, where the information transmitted in different bands is the same. Nevertheless, frequency hopping is used in response to the channel's scattering function whereas diversity is used to overcome frequency selective fading.

modulating several carriers with the same information signal. Another method for this purpose, is to use different time slots (time diversity). In the former, the frequency separation must be higher than the inverse of the total multipath spread (coherence bandwidth), whereas in the latter, the time spacing must exceed the inverse of the Doppler spread (coherence time)[6]. This is due to the need of assuring that fading in different channels is, in fact, uncorrelated. Of course, the use of these forms of diversity implies a trade-off between bandwidth efficiency and robustness, which may be critical due to the lack of bandwidth in underwater acoustic channels. Frequency diversity can also be easily obtained through the use of DSD modulations [13], since it is a natural consequence of the data signal's power spectrum being replicated around the carrier's frequency. These explicit forms diversity obviously consist of a redundant use of the available signal space (the time and frequency spans of the signal). However, the so-called implicit diversity can be obtained by resolving each of the multipath components and combine them coherently to better estimate the transmitted signal[7], without the mentioned redundancy.

Another important form of diversity commonly used in underwater acoustic communications is spatial diversity, where an array of transducers properly spaced at the receiver allows for the reception of uncorrelated signals. Unlike the other forms of diversity, this one has the interesting property of not requiring a higher bandwidth consumption[7].

Altogether, the benefits of explicit diversity usage among many developed systems are somehow speculative. This is due to the lack of measurements of the medium's coherence time or bandwidth for the actual deployment scenarios, as without them it is impossible to ensure an effective use of uncorrelated channels. To that end, [15] estimates such measures for specific channels and concludes that the coherence time is actually frequency dependent.

Coding

Channel coding is another way of achieving higher reliability, through the insertion of redundancy in the bit stream (of course, at the cost of reducing the information data rate). In the underwater acoustic telemetry, the most commonly used codes are the block and convolutional ones.

Conceptually, coding has important similarities with diversity usage. In fact, if coding a data sequence results in its spread over an amount of time greater then the coherence time of the channel, a form of time diversity is provided. This principle may be transposed to frequency, as coding methods may be applied to the selection of tones in MFSK so as to introduce a controlled amount of redundancy - a technique termed coded modulation [16]. The benefits of this technique were explored in [12], with the use of an Hadamard code.

[6] The interested reader should refer to [8] for a complete deviation of such measures.

[7] As stated in [14], "Information theoretic studies have shown that the capacity of a channel increases linearly with the minimum of the number of transmit and receive antennas".

2.3.2 Techniques for active multipath and Doppler compensation

In order to actively mitigate the ISI caused by multipath, receiver designs specially developed for that purpose may be used. As such, [8] derives an optimum[8] ML receiver for the generic ISI affected channel, whereas [1] derives a similar one for the case in which the receiver features a sensor array and thus benefits from spacial diversity. The defining characteristic of both receivers is the fact that they use a matched filter in conjunction with MLSE to decide which sequence was effectively sent by the transmitter, thus they exploit the implicit temporal diversity resulting from ISI. This implies a trellis-based analysis through the use of the Viterbi algorithm. Since the computational complexity of MLSE grows exponentially with the number of symbols spanned by ISI, in most underwater acoustic channel, it becomes impractical. On the other hand, the time-variable nature of the channel combined with the absence of an a priori knowledge of its impulse (or frequency) response, implies the use of suboptimal adaptive equalizers that are both adjustable to it and adapted to its variability.

Adaptive equalization

Adaptive equalization can be performed by linear or nonlinear equalizers whose parameters, namely its filters coefficients, are adaptively adjusted to the channel's characteristic through the use of a training sequence transmitted from time to time. Both approaches will now be presented[9].

Linear equalization may be implemented through the use of a simple FIR filter[10]. This is usually done by the generation of an error signal that adjusts the coefficients based on the difference between decisions previously made by the detector and the actual sent symbols (those of the known training sequence). Several criterion may be used for this adjustment.

The most common criterion is the minimization of the MSE between the mentioned symbols. Such minimization is usually accomplished through the use of the LMS or the RLS algorithms. Selecting one of these implies a trade-off between low implementation complexity (LMS) and fast convergence (RLS). Nevertheless, there are as well implementations of the latter that provide a reduction in its computation complexity.

It is important to point out that these equalizers are not suited for situations where some frequencies are strongly attenuated, as is the case of many multipath fading channels. This is due to the type of compensation provided in such cases, which consists of a large spectral gain in the fading frequencies, resulting in an enhancement of the noise component of the received signal.

The second type of equalizers resorts to nonlinear operations to compensate for channel distortions too sever for linear equalizers. The most common form is the decision feedback equalizer (DFE) and its main idea is to use previously detected symbols to estimate the ISI that these will cause in the following symbols and subsequently remove it.

[8] Optimum from a sequence estimation error point of view.

[9] An extended analysis is exposed in [17].

[10] IIR filters are seldom used due to the possibility of the poles moving outside the unit circle during the adaptation process.

To do so, these equalizers use an additional filter - the feed-back filter - whose coefficients are adjusted in order to cancel the ISI that past detected symbols will cause on the current symbol. Since this particular filter is linear[11], its coefficients are usually adapted through the use of a linear algorithm such as the RLS or LMS.

As happens with the previous type of equalizers, there are several implementations of nonlinear equalizers with variable computational complexity. Despite their susceptibility to error propagation, nonlinear equalizers are significantly more robust then their linear counterparts. Therefore, they are appropriate for very harsh channels, such long horizontal links and consequently, are often the chosen to perform adaptive equalization in underwater acoustic systems.

In order to reduce the computational complexity of adaptive equalization, the sparse nature of the channel can be exploited through the use of sparse equalization. This technique consists of the reduction of the number of equalizer taps, keeping only those regarding significant multipath arrivals. Consequently, besides the complexity reduction, sparse equalization allows for faster channel tracking and improved reliability since the noise between multipath arrivals is not processed.

In order to avoid the use of training sequences, one can resort to blind equalization techniques, which rely only on statistical properties of the signal. Naturally, these suffer from a slower convergence which might be prohibitive considering the channel's temporal coherence.

An important mechanism to improve the DFE's resilience to error propagation is turbo equalization. It consists of a joint estimation, equalization and decoding, as the decoder is included in the DFE's feedback loop. Several methods regarding sparse, blind and turbo equalization are briefly discussed in [14].

A widely used adaptive equalization scheme derived from the optimal ML with spacial diversity was proposed [1, 18]. Its structure is presented in figure 2.3. This structure combines a DFE to equalize the slowly varying channel response with a second order digital PLL to track the more rapid phase fluctuations caused by the Doppler effect, jointly optimized over MSE. The success of this implementation is given to the vulnerability of both techniques when optimized separately[19]. More specifically, the existing time-varying ISI makes phase tracking almost unfeasible (as was discussed throughout the present chapter), whereas phase fluctuations due to Doppler and multipath affect significantly the equalization's performance[12].

The evolution of this canonical receiver throughout the years has been towards the reduction of computation complexity and the increase of robustness. Some examples of such attempts are summarized in [2]. The latter has been achieved with the use of Doppler shift compensations in order to ease the tracking task of the DFE-PLL.

[11] Although this filter is linear, it is used in combination with the other one (the feed-forward filter) and thus the resulting operation is nonlinear.

[12] Nevertheless, the coupling between the DFE and the PLL may become unstable[20].

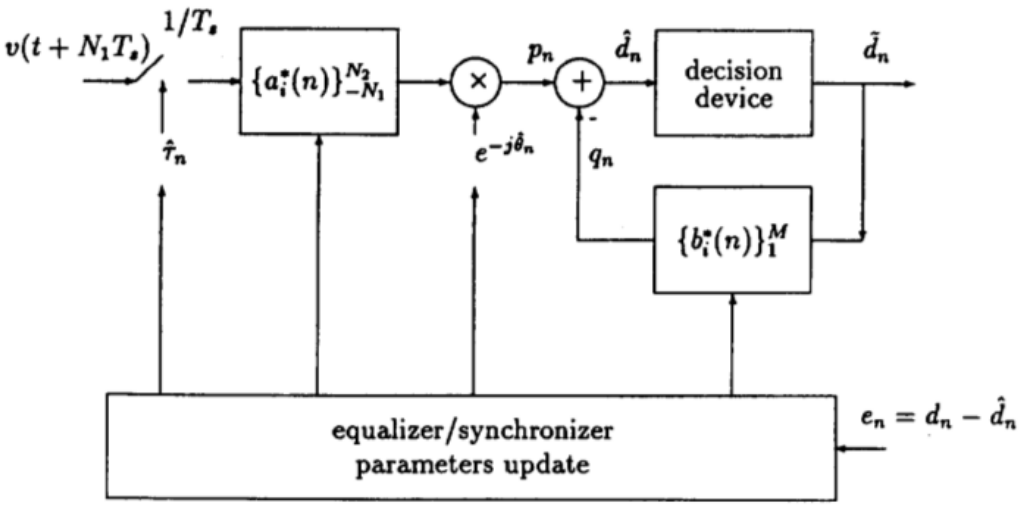

Figure 2.3: Canonical coherent receiver proposed in [1].

Doppler compensation

Since the Doppler effect corresponds to a scaling of the signal, if the actual scaling factor is known, it can be effective removed by performing the inverse operation. Many papers claim to use such technique with great effect either by performing a digital resampling or by acting on the ADC sampling frequency. Of course, techniques for estimating the amount of motion are required [21].

2.3.3 Simulations

Throughout the years, many researchers have used simulations in the development of their systems. While these are a powerful tool for assessing signal processing algorithms, they cannot be used for a thorough evaluation of the entire system. This is due to the lack of incorporation of all the important factors of the channel in a single simulator and the variability these factors experience among different channels. For instance, many simulators do not account for the time variability, which is of course a defining characteristic of the channel. Additionally, many rely on pure ray propagation which is not appropriate for modeling the scattering phenomenon. Nevertheless, recently, there has been an increase in the quality of developed simulator. One of the most sophisticated is presented in [22].

2.3.4 Modulation schemes

Incoherent modulations

The use of these modulations is a common and well known means of avoiding the mentioned reverberation issues, even without complex signal processing algorithms, and consequently, high processing power. However, these suffer from the high bandwidth they require, as their spectral efficiency is limited to 0.5 bits/Hz. In fact, these receivers are much more appropriate for power

limited channels than for band limited ones. This makes incoherent systems unsuited by nature to underwater acoustic channels, specially for the case of high data rate applications. Therefore, these are mostly used in very harsh environments, like horizontal links on shallow waters, when moderate data rates are required.

Since the frequency of the signal is its most unchanged property after passing through this channel (even with the associated Doppler effect), FSK based modulations are the most widely used modulation scheme in this type of receivers. Furthermore, these provide a threshold-free decision, since the receiver just needs to select the tone with the highest energy.

This receivers often employ a bank of narrow band filters, using the energy detected at the corresponding outputs as a means of deciding which of the possible frequencies was sent. One common practice is to do so by computing the received signal's FFT. In some cases, in order to account for the Doppler shift, the narrow bands of this filters are modified, as well as the carriers used for demodulation. Common strategies for improved reliability include diversity usage (in some cases with frequency hoping) and guard intervals.

The earliest of these systems had very low bit rates, due to hardware limitations and also because the data to be transmitted did not require higher rates [10, 23, 24]. Nevertheless, these were highly reliable as they already used techniques such as diversity and guard times.

In order to improve the bandwidth efficiency, some FSK extensions may be used, such as multiple tone FSK (MT-FSK) [23, 13, 12], which consists of sending more then one tone simultaneously. This enlarges the alphabet[13] (whose length is of course equal to the number of tones in regular FSK) and thus allows to reduce symbol time for a given information rate at the cost of reduce error robustness (for a fixed average energy). The latter can be improved by selecting only a subset of all possible tone combinations as a way of increasing the Hamming distance between symbols (thus implementing a sort of diversity). There are also techniques based on more complex selection of the possible tone combinations [25], with the goal of increasing energy and bandwidth efficiency on specific channel models.

Coherent modulations

This receivers emerged in the 90's in response to the growing demand for high data rate systems, after being confined to vertical links on deep waters and considered unfeasible in the remaining situations for decades. Their efficient spectral usage goes far beyond what could be expected from incoherent systems, however, they lack an inherent robustness up to the requirements of underwater acoustic communications. Instead, they rely on more sophisticated techniques, such as adaptive equalization and Doppler estimation, whose goal is to actively mitigate the these undesirable effects, in order for the phase to be properly tracked by the receiver. Unlike the previous type of receivers, this one undertook major developments in the last decades.

The use such receivers arose from the use of DPSK modulations, which were not exactly coherent, but served as a preliminary step to the use of phase information rather then frequency

[13] Some authors prefer to describe it as different channels, each with a regular FSK modulation.

information of the signal. In fact, these were much easier to implement, since they did not need an explicit estimate of the carrier's phase, however, they suffered from a higher error probability[14], when compared to their purely coherent counterparts. Nevertheless, the effect of increased bandwidth efficiency was clear, as even one of the first implementations of DPSK [26] allowed for a data rate of 4800 bit/s at a 45°angle, which was considerably higher than what was usually achieved by incoherent systems.

Multi-carrier modulation

Multi-carrier modulations, namely OFDM, have several desirable properties that render them an interesting alternative to single-carrier modulations in underwater acoustic communications. First of all, OFDM is robust by nature to the two main consequences of multipath: protection against ISI through the use of guard intervals (often implemented as cyclic prefixes) does not compromise the data throughput due to the low symbol rate whereas the frequency selective fading is easiest to cope with since fading remains approximately constant over each sub-band. Furthermore, equalization is greatly simplified as it can be performed on the frequency domain. Finally, modulation and de-modulation can be efficiently implemented with the FFT.

On the other hand, such modulations are much more sensible to the Doppler effect[27, 4], as even small Doppler shifts will be on the order of the carrier spacing, causing a distortion that can not be seen as equal to all sub carriers. In other words, the Doppler shifts will be severe and the Doppler spreads cannot be neglected due to the wideband nature of the modulation.

2.4 Brief description of some systems

It is important to perform an analysis of particular systems, mainly those of greater relevance to the course of the field. This discussion will mainly consist on incoherent FSK systems, as these have greater resemblance to the system to be developed.

One of the first attempts to actively compensate for multipath was presented in [28]. This seminal work relied on the use of signals consisting of an impulse, which allowed to measure the channel's impulse response, followed by an hyperbolic FM sweep (the information signal) with Doppler invariant correlation properties. An estimation of the information signal was obtained through the cross correlation between the received signal and the measured impulse response. From this description it is clear that this work benefited from the channel's temporal coherence (which was of course larger than the total duration of the used signal), an approach followed by researchers thereafter.

One of earliest implementations of incoherent modulations is presented in [10], where a system for the transmission of control data from a ship to some small submersibles at medium or high depth, with a minimum distance of 100 nmi, is proposed. In this work, a 4-ARY FSK modulation was used, with multipath and Doppler protection through the use of long pulses, large frequency

[14] Or, equivalently, smaller power efficiency.

spacing and 5 diversity channels. In order to achieve low error probabilities, a Golay code was used. Doppler estimation was also performed, through the use of a two phase preamble. Although Morgera only simulated this design, it was later submitted to experimentation, achieving a 40 bits/s at a depth if 50 m and a distance of 2 nm in quiet waters.

One of the first successful implementations of MT-FSK is proposed in [23]. In this design, Wax used 16 tones, each pair of which representing a bit (8 simultaneous tones). For improved reliability, 4 diversity bands were used, as well as guard times in each diversity band. In order to maintain a constant power envelope, each of these bands was transmitted in a different time slot (time-hopping). Additionally, ARQ was implemented through the use of a feedback channel, since FEC encoding allowed the receiver to detect errors.

Another important implementation is the DATS system [11]. It uses MT-FSK with up to 16 simultaneous tones in the interval $[45;55]$ kHz. These were synthesized by a frequency generator controlled by a microprocessor according to the input bitstream, and frequency hopping was used in order to have avoid the lack of efficiency of guard times. Additionally, the system sent a continuous 60 kHz tone to be used for Doppler estimation and also a short pulse centered at 30 kHz to signal the beginning of each data word. At the receiver side, it separated the three components with bandpass filters. A Doppler estimator derived through the use of a PLL was used to determine the frequency of the carrier to be used in the demodulation stage. The system achieved data rates of up to 1200 bits/s including redundancy.

One of the first successful implementations of a purely coherent receiver design on representative underwater channels is presented in [1, 18]. This seminal work, whose receiver design was already presented in figure 2.3, proved that coherent modulations were feasible, even in horizontal channels, through the use of a joint carrier synchronization (PLL) and channel equalization (DFE) with RLS coefficient update. This PSK system, which benefited from spacial diversity, achieved an impressive data rate of 1000 bits/s on a challenging 90 km shallow water horizontal channel with error rates lower than 10^{-4}. This design became a standard for coherent receivers as several systems presented subsequently were based upon the same principals [2].

Chapter 3

The previously developed FSK modem

As was previously mentioned, the modem will be built on top of a previously developed fundamental structure - an FSK modem. Prior to the definition of strategies for the enhancement of this system, it is essential to study it, so as to gain insight into its implementation details and, above all, the most critical aspects of its performance. To that end, in this chapter a description of this system will be presented.

3.1 System description

3.1.1 Overview

The system can be divided into the analog front-end which receives the signals directly from the transducers and performs all the pre- and post-processing stages, including the A/D and D/A conversion, and the development board which contains an FPGA where the digital side of the modem was implemented, as presented in figure 3.1.

Transducers

The piezoelectric transducers [29] are used for both the reception and the transmission of the acoustic signals, and their interface also includes an electric circuit specially developed to perform the necessary voltage transformations and impedance matching [30]. The most defining characteristic of these devices is their narrow frequency response, which is presented in figure 5.1. This factor imposes important limitations to the bandwidth of the transmitted/received signals.

Analog front-end

The analog front-end [31] contains a reception and transmission circuit. The former includes several pre-amplification stages and variable gain amplifiers, an anti-aliasing (AA) filter with a cutoff frequency of 250 kHz and a 12-bit ADC with a maximum sampling rate of 1

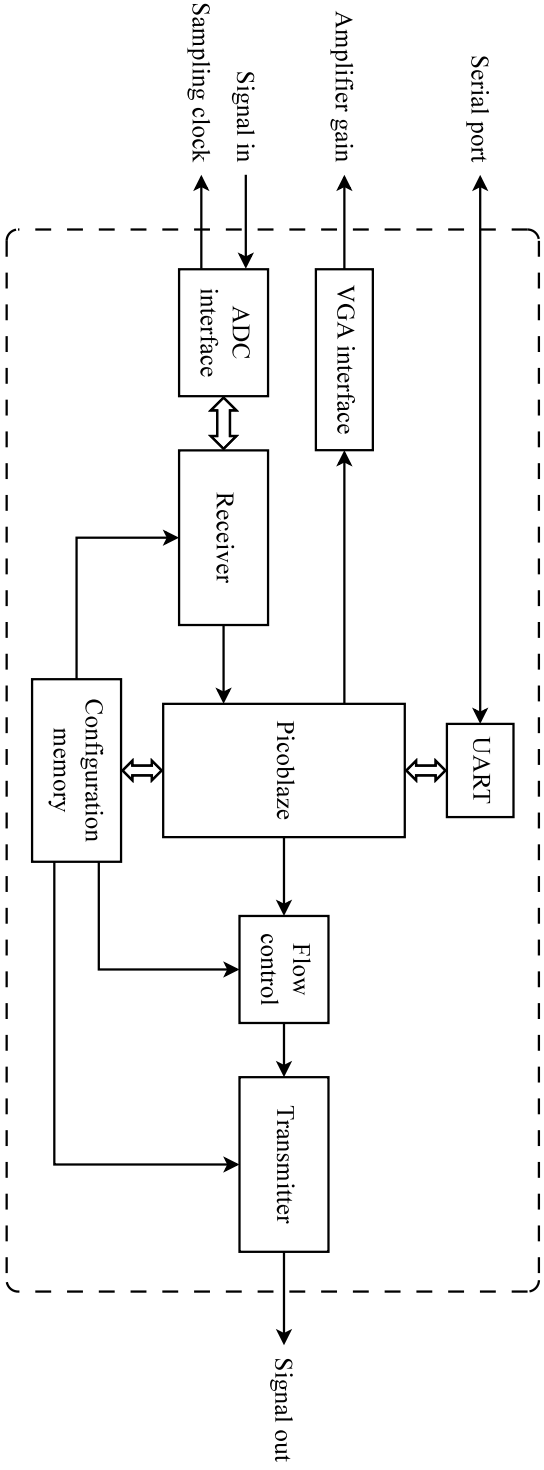

Figure 3.1: Overview of the general architecture of the previeously developed system [3, p. 16].

Msps. The latter contains a low-pass filter for the digital-to-analog conversion[1] followed by an audio amplifier [32] whose output is fed to the circuit that interfaces with the transducer.

GODIL board

The GODIL board [33] is a prototyping tool based on the Xilinx Spartan-3E FPGA [34] which includes an SPI flash memory to store its configuration bitstream and a local 49,152 MHz oscillator.

FPGA

The core of the modem is implemented in the FPGA. Its clock rate of 98,304 MHz is derived from that of the local oscillator through the use of a PLL. The system interfaces with a computer through a serial protocol implemented by a UART module, which is used to exchange control information as well as the bit streams. To ease this process a command line interpreter with several useful commands was implemented. The receiver side contains an ADC interface, which receives the converted signal and controls its sampling rate, the VGA interface and the receiver itself. The transmitter side contains a flow control module that sends the bit stream to the transmitter at a constant rate and the transmitter itself. The main control tasks (which are not time critical) are performed by a soft-coded Xilinx Picoblaze [35], which interfaces with the UART module and writes to the registers that are read by the other blocks for configuration purposes during the device's operation. Since the goal of this dissertation is to enhance the performance of this system in regards to its robustness and data rates, our effort will be mostly directed to the receiver and the transmitter, therefore, it is important to analyze these blocks with more depth. Although the following description aims to present all the relevant aspects of this system, the interested reader can refer to [3] for the complete analysis thereof.

3.1.2 Transmitter

The transmitter comprises several blocks the act in series, i.e. each one processes the data that was outputted by its predecessor, as is presented in figure 3.2. The transmission chain begins with the channel coding block (which was not actually implemented) and the S/P block which converts serial data at a constant rate (the transmission bit rate) to parallel according to the number of bits per symbol[2] followed by the mapper which performs the symbol mapping in a Gray fashion. The frequency generation is performed by a DDS core [36], which is basically an accumulator that receives a phase input - the phase increment - and a sine/cosine lookup table which is indexed with the generated phase itself, therefore, the phase input directly controls the generated frequency. This ip core is highly parameterized, however, the most relevant parameter of its current configuration is its frequency resolution - 93,75 Hz. In order to perform the conversion from symbols to phase increments the transmitter also includes the modulator, which does so by the means of a lookup

[1] As will be explained below, the outputted digital signal is sigma-delta modulated, therefore, this conversion can be performed using only a low-pass filter.

[2] In this configuration this value corresponds to the base-2 logarithm of the number of symbols.

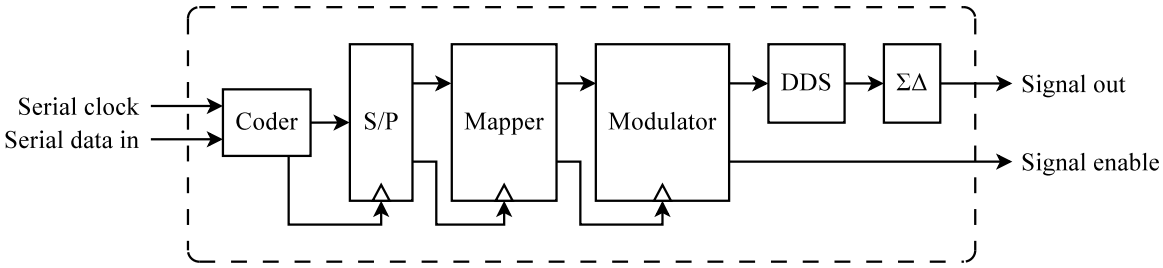

Figure 3.2: Overview of the architecture of the previeously developed transmitter [3, p. 18].

table and is also in charge of controlling the symbol timing. Finally, the generated digital sine wave is sigma-delta modulated by the last module.

3.1.3 Receiver

The most defining characteristic of the receiver is the fact that it is based on the DFT, as shown in figure 3.3. The processing chain starts with a polyphase decimator FIR filter [37] with pass band $[19;29]$ kHz, which lowers the sampling rate to 96 kHz and filters the noise outside this interval. Unlike many papers mentioned in the previous chapter, no downconversion is performed.

The resulting signal is stored in a buffer so it can be randomly accessed, as is required when there is overlap in the DFT computation, whose size is fixed at 256 points[3]. In order to avoid the hardware requirements of the computation of the absolute value of a complex signal, the absolute values of the DFT are approximated by

$$\alpha Max + \beta Min \Big|_{\substack{\alpha=1 \\ \beta=\frac{3}{8}}}$$

where Max and Min are the maximum and minimum absolute values among the real or imaginary parts of all DFT points, respectively [39].

After the DFT computation, the equalization module computes a factor for each symbol (frequency) according to its amplitude in the preamble (Sec. 3.1.4) and multiplies the subsequent amplitudes by that factor, so as to compensate for the channel's and transducers' response. Once again, for resource efficiency purposes, the factors are powers of two. Based upon the values outputted by this module, the acquisition and timing blocks trigger the start of the reception and the sampling instant, respectively. However, the latter basically just counts the number of samples per symbol, as no timing tracking mechanism for operation during the actual data transmission was implemented. Consequently, although a Doppler estimation algorithm was proposed, it was also not implemented as it depended on the timing tracking module.

Finally, the demodulator chooses the symbol whose bin is closest to that of the maximum absolute value of the DFT, and the remaining modules perform the inverse operations of those of their counterparts at the transmitter.

[3]For baud rates in which each symbol corresponds to less than 256 samples, the input is zero padded in order to perform a DFT interpolation [38].

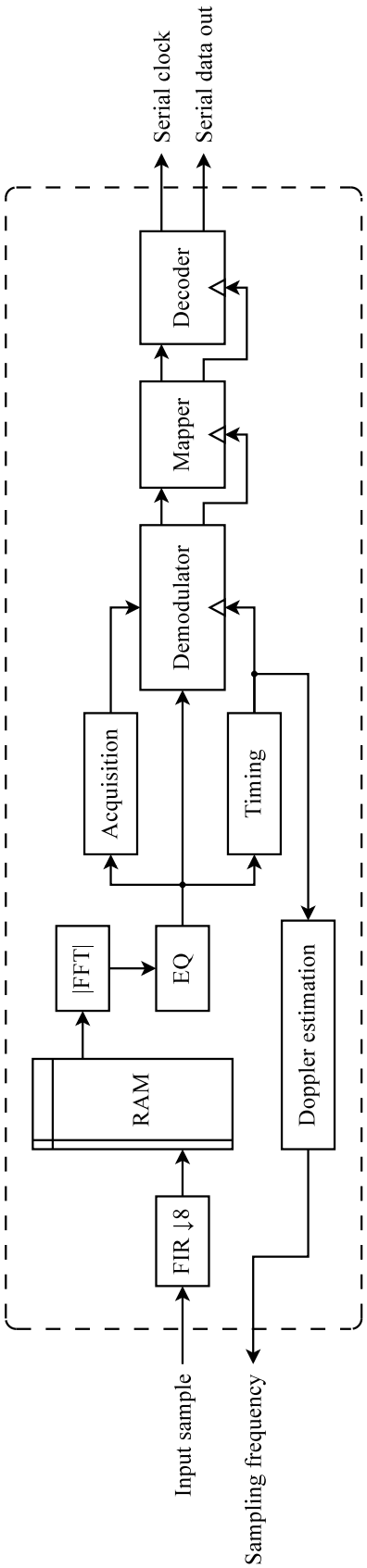

Figure 3.3: Overview of the architecture of the previeously developed receiver [3, p. 20].

3.1.4 Operation details

Frame sequence

The communication is based on frames, which comprise a header and the actual data. The former has the following structure:

1. *Acquisition tone* - A tone that spans through several symbol intervals and is used to signal the start of the frame and to compute its equalization factor.
2. *Equalization starter* - A second tone that is sent during 2 symbol intervals for the purpose of the computation of its own equalization factor.
3. *Synchronization preamble* - A sequence of the former tones alternating at a symbol time basis that is sent throughout several symbol intervals for purpose of synchronization.
4. *Equalization tail* - The remaining symbols (if there are any), are sent for equalization purposes.

Frequency Acquisition

The algorithm that identifies the start of a new frame and triggers the reception process is based upon the detection of a tone above the noise (the acquisition tone) in the DFT domain. As such, the noise level is continuously estimated by the means of an exponential moving average and compared with the maximum absolute value among all DFT bins. Depending on these two quantities and a set of fine-tuned constants, the algorithm determines weather lock is acquired (the decoding process starts) or lock is lost (the decoding process finishes). The correct bins are estimated through a voting process for a reduced area of implementation. The DFT is computed with an overlap of 50% in order for the acquisition tone to be short. Further details can be found in [3, Sec. 4.3.4].

Initial synchronization acquisition

The initial synchronization is based on an algorithm presented in [40, 41] whose basic idea is that upon symbol transitions, if the DFT is computed with a sufficient amount of overlap, the amplitudes of the corresponding bins can be used to determine whether the receiver's delay is positive or negative and thus provide an estimate of the right sample instant. Such procedure takes place during the synchronization preamble, hence its symbol transitions, and best overlap is chosen through a voting system. Further details can be found in [3, Sec. 4.3.6].

3.2 Reported results

The reported tests were performed in a marina and also off-coast. In regards to the former, only the best result is mentioned: a BER of $3,4 \times 10^{-3}$ at distance of approximately 5 meters, a baud

Figure 3.4: Bit error pattern obtained in off-coast experiments [3, p. 18].

rate of 750 symbols/s and a data payload of 2048 bits. Although this result itself does not provide much information on the main cause of errors, based on a presented DFT bin histogram that shows very little variance around the bins of interest, the author suggests the errors occur mainly due to multipath. The off-coast results, in turn, offer more insight into the nature of the errors: at a distance of approximately 50 meters, a baud rate of 375 symbols/s and the same data payload, the error pattern presented in figure 3.4 was obtained, which corresponds to a BER of $1,91 \times 10^{-1}$. The author states this error pattern is most likely due to motion induced Doppler, as with a relative speed of 0,75 m/s the synchronization acquired during the sync preamble would be lost after approximately 250 symbols and the communication would be completely unreliable thereafter, as is the case. Regardless of this severe effect, the first 250 symbols prove that the channel is quite clear, as is expected due to the lack of obstacles and low tendency to generate multipath.

Chapter 4

Preliminary tests

Although the results reported in [3] were somehow enlightening in regards to the off-coast environment, an accurate selection of enhancement strategies perfectly fitted to the system required a more in-depth study of its performance. Therefore, a new set of tests was specially developed for this purpose and conducted prior to the any modification to the previously developed system.

4.1 General methodology

4.1.1 Setup

The data transmission was performed by the actual hardware platform and the results were recorded by a digitalHyd SR-1 [42], with a sampling frequency of 101,562 kHz and a resolution of 24 bits. The recorded signals were then analyzed in the MATLAB environment, as the hardware implementation in Verilog HDL did not offer the required debugging capabilities. As such, the receiver algorithm was implemented in this environment with a high degree of fidelity.

4.1.2 The Short-time DFT analysis

In order to evaluate the received signals, besides computing the number of errors[1] and observing the corresponding DFTs, we decided to use an approach similar to that of [40] - a short-time DFT (ST-DFT) analysis. More specifically, we found that the plot of the absolute value of the DFT bins of interest along time, with some amount of overlap, was a powerful tool for a rapid and qualitative assessment of the received signals. This is mainly due to the temporal information provided by such measure, which allows us to draw important conclusions as will become evident throughout this dissertation. More specifically this measure can be defined as

$$X[k,m] = \sum_{n=0}^{N-1} x[n+m]w[n]e^{\frac{-j2\pi kn}{N}} \tag{4.1}$$

[1] According to the receiver replica implemented in MATLAB.

where m is the start index of the signal section to be transformed, $w[n]$ is the window function and N is the DFT size[2]. This measure naturally implies an overlap factor of $1/N$ between consecutive m indexes, however, as such resolution might be too high, it is important to consider other factors. Hence, for the generic case of an overlap factor of O, m will take the set of values $i(1-O)S, i \in \mathbb{Z}$, where S is the symbol size. There are, therefore $1/(1-O)$ computations per symbol, or in other words, the symbol size in the ST-DFT domain is equals $1/(1-O)$. Consequently, a simpler notation for this particular application would be

$$X_i[k] = \sum_{n=0}^{N-1} x[n + i(1-O)S]w[n]e^{\frac{-j2\pi kn}{S}}. \tag{4.2}$$

As for the the actual overlapping factors, we found $15/16$ to be appropriate for the mentioned qualitative analysis.

The methodology here described applies to all the experiments presented throughout this document unless specified otherwise.

4.2 Oceansys tank

The first set of tests was performed in a faculty's tank ($4,60 \times 4,80 \times 1,80$ m), as the availability thereof and short setup time required was suited for initial experiments. However, this medium was of course expected to be unrealistically reverberant when compared with the actual deployment scenarios, therefore, some sort of measure of the channel's response to acoustic signals was necessary before any transmission attempts were made. More specifically, such measure should provide some insight into the structure of the multipath, namely, its extension in levels similar to those of the first replica.

4.2.1 The channel's response

Since the available equipment was not capable of transmitting short pulses whose temporal span was short enough to cover all the bandwidth of interest, another approach had to be followed. To that end, several experiments consisting of the transmission of single symbols with several parameter combinations were made, as the results would allow us to estimate how a symbol was time spread into the following symbol intervals. For this experiment as well as for the upcoming ones, the transmitting transducer and the sound recorder were at the center of the tank with a separation of about 1 meter. The results were then analyzed through the mentioned ST-DFT method. One such result is presented in Fig. 4.1.

Before drawing any conclusion based upon this figure it is important to keep in mind that the multipath's nature is, as discussed previously, time- and frequency-dependent. Although the former dependency should be negligible in such a static environment, the latter plays an important role, as was proved through experiments. Therefore, this figure does not represent the multipath's

[2] A general analysis of this subject can be found in [38, Ch. 10]. For a more deep in-depth discussion, refer to [43].

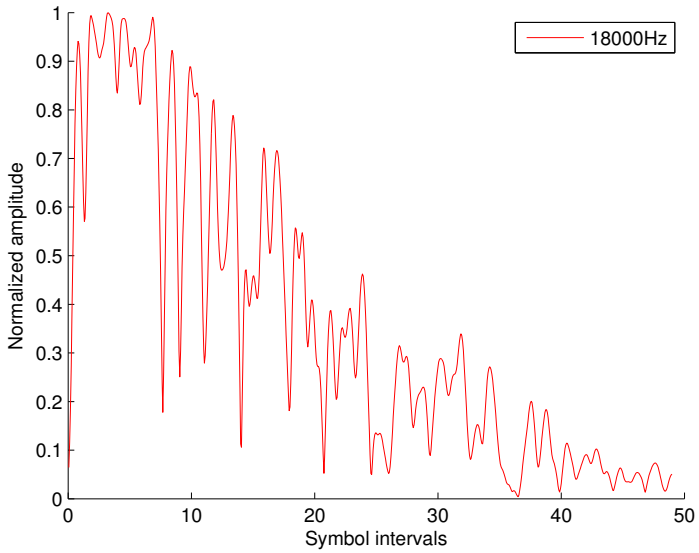

Figure 4.1: Normalized absolute value of the 18 kHz DFT bin along time upon the transmission of single symbol in that frequency at the tank. Relevant parameters: 750 symbols/s baud rate, 256 point DFT, an overlapp factor of 15/16 and 80 out of 255 transmission gain.

structure in all frequencies. It does, however, provide qualitative and approximate measure of the overall multipath's extension, and thus meets the requirements of this experiment.

Hereupon, from this figure one can see the first replica (the first peak) and a tremendous amount of reverberation thereafter. Since the amplitude of the latter only drops to half of that of the former after about 20 symbol intervals[3], it becomes clear that transmitting a second symbol during that time span would render the communication completely unreliable. Experiments with other frequencies and baud rates indicated similar values of the total multipath span, which proofs the representativeness of this measure.

4.2.2 On the relationship between the gain and the resulting multipath structure

Before giving up the transmission in such a harsh environment (at least without the mentioned structural modifications), a final test based on a rather intuitive idea was performed. It consisted of conducting these experiments with different transmission gain values, so as to determine the impact of this factor in the total multipath span. The results are presented in Fig. 4.2, where the image of Fig. 4.1 has been included for the purpose of comparison.

As it can be seen, the results indicate that the amount of reverberation, as measured by the ratio of its amplitude to that of the first echo and also its time span, increases with the amplitude of the transmitted signal. Despite being intuitive, this outcome proofs that the channel is actually highly non-linear, most certainly due a combination of the transducers' sensitivity and the attenuation of

[3]In the case of this particular frequency, the amplitude of the echos during the first symbol intervals is actually higher than that of the first replica.

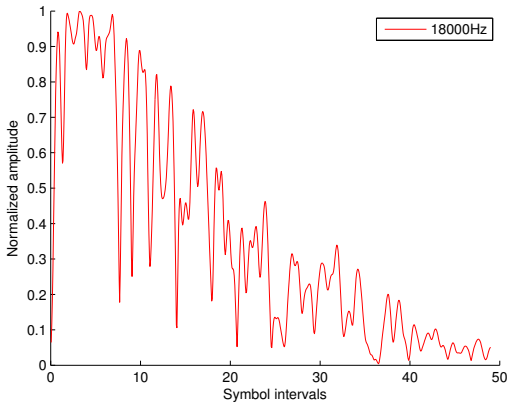

(a) 80/255 transmission gain (Fig. 4.1).

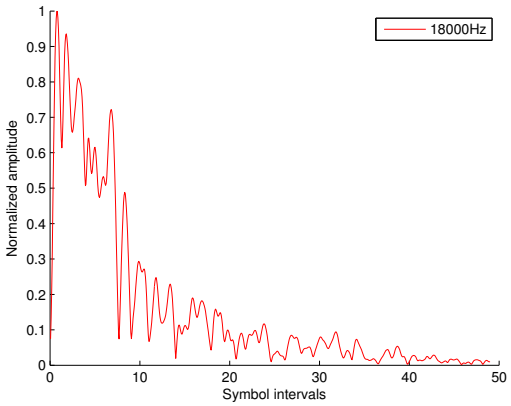

(b) 20/255 transmission gain.

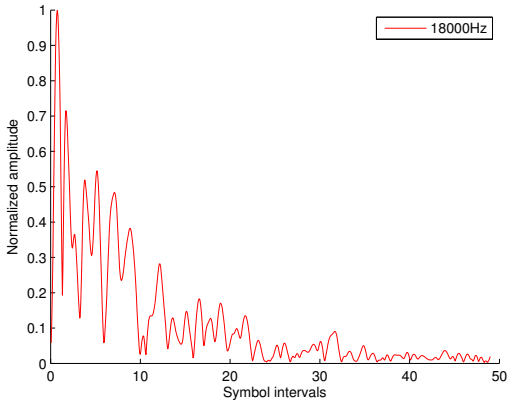

(c) 14/255 transmission gain.

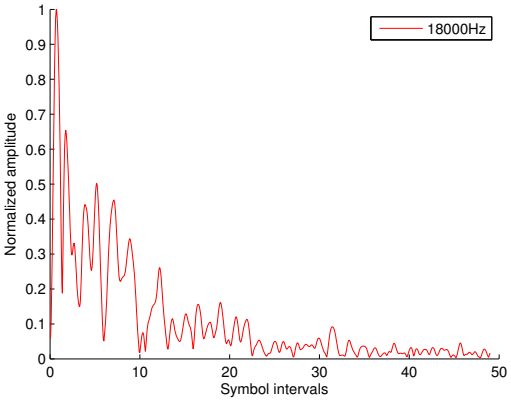

(d) 10/255 transmission gain.

Figure 4.2: Normalized absolute value of the 18 kHz DFT bin along time upon the transmission of single symbol in that frequency at the tank for different transmission gains. Relevant parameters: 750 symbols/s baud rate, 256 point DFT and an overlapp factor of 15/16.

the medium (Eq. 2.2.1). Nevertheless, it can be concluded that a fine-tuned transmission gain has an important impact on the reliability of the communication.

4.2.3 Experiments with a fine-tuned gain

With the last result in mind, several experiences with longer sequences and a fine-tuned gain - 12 out 255 - were conducted. A segment of a representative result is presented in Fig. 4.3.

Probably the most noticeable aspect of this figure is amplitude difference between the frequencies - a ratio of about 3/2. Although the multipath structure of each individual frequency also contributes to amplitude fluctuations, such noticeable difference is most certainly due to the transducers' response as well as that of the remaining electric circuit. Although the equalization at the receiver partially addresses this issue[4], the "fine-tuned gain" strategy is compromised by

[4]Although Fig. 4.3 shows the amplitudes prior to equalization, the latter was performed in the decoding process, otherwise the BER would have risen to $3,125 \times 10^{-1}$.

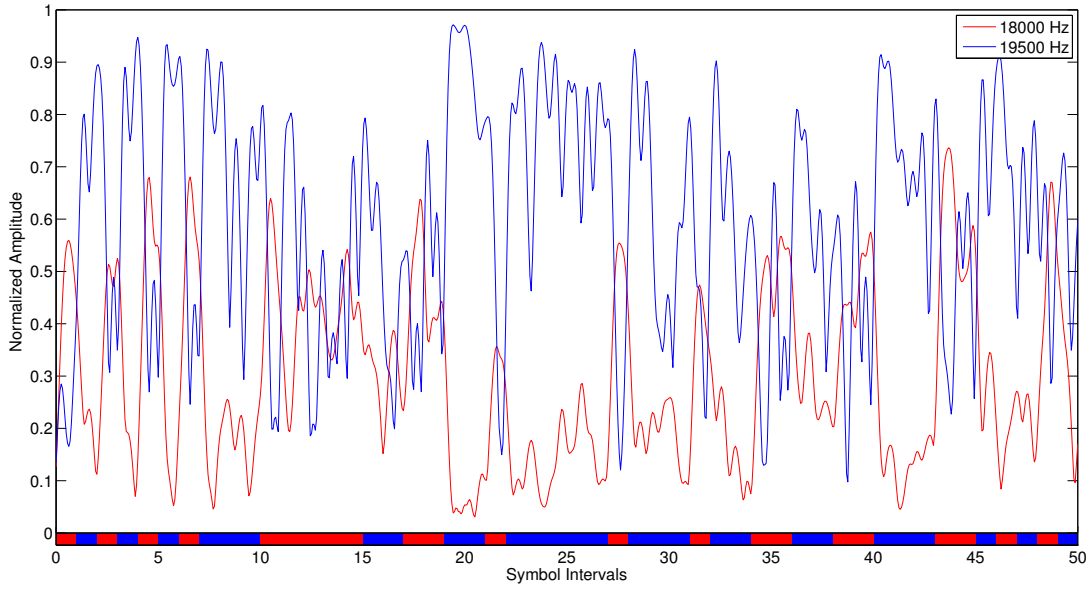

Figure 4.3: Normalized value of the relevant DFT bins along time (above) and the sent sequence (below) upon the transmission of 4096 bits at the tank (only the first 50 bits are shown). Resulting BER: $2,422 \times 10^{-1}$. Relevant parameters: 2 tones (BFSK), 750 symbols/s baud rate, 256 point DFT, an overlapp factor of 15/16 and 12/255 transmission gain.

such amplitude differences. In fact, the higher amplitude of the 19,5 kHz sine wave, results in a heavier multipath structure, as becomes clear in the intervals [10;15] and [45;48]. On the other hand, although the amount of reverberation produced by the 18 kHz sine wave is lower, it still precludes the establishment of a reliable communication. Therefore, strategies to cope with heavy multipath environments must be considered.

The mentioned amplitude difference can also be observed in Fig. 4.4, where the average value of the DFT bins throughout the transmission is presented. This figure also shows an unexpected peak near 25 kHz, which is most lost likely a noise induced oscillation, since it is near the transducer's resonant frequency. However, besides this small peak, the channel is actually noiseless, as one would expect.

Besides this reasoning, Fig. 4.3 allows for one final remark of extreme importance. It can be seen that the first eight bits correspond to a sequence of alternating symbols, as is the case of the sync preamble. From the severe amplitude fluctuations of the 19,5 kHz wave and, most importantly, the low amplitude difference between the waves when the 18 kHz symbol is sent, one can immediately conclude that this algorithm is very prone to errors. Therefore, a careful consideration on whether to keep this sync algorithm must be made.

4.2.4 Measurement of the output circuit's response

The previous results indicated a strong frequency dependency of the transmitted power. Although such relationship was already measured in regards to the transducers [29], there is no record of the measurement of the frequency response of the output electrical circuit. In order to estimate it, a

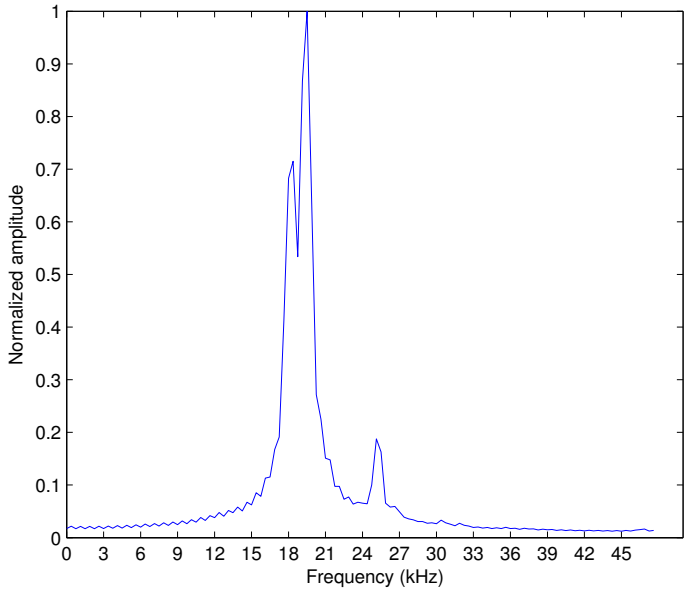

Figure 4.4: Normalized average value of the DFT bins throught the transmission of 4096 bits at the tank. Relevant parameters: 2 tones (BFSK), 750 symbols/s baud rate, 256 point DFT, an overlapp factor of 15/16 and 12/255 transmission gain.

final experiment consisting of the measurement the voltage applied to the transducer's terminals upon the transmission of the 53 equally spaced tones in the [15;34.5] kHz band was conducted. The normalized result is presented in Fig. 4.5.

Although the depicted response may appear unexpected, it might actually explained by the elements the circuit comprises: a low-pass filter with a cutoff frequency near 45 kHz (the sigma-delta demodulator), a band-pass filter with pass band [14; 15000] Hz (the audio amplifier) and the transmission circuit which was designed to perform impedance matching around 23 kHz. Determining whether these are the actual causes of such behavior was out of the scope of this dissertation, as it required a more careful analysis thereof and we are more interested in the response itself. Therefore, there was not enough information for data fitting to be performed, however, as will become apparent in the following chapters, the measured response values are perfectly adequate for the their application in the forthcoming work. Regardless of this reasoning, it is important to note that the response quite sharp (on the order of that of the transducers), therefore, it cannot be neglected.

This experiment also provided an estimate of the apparent power at the transducer's terminals at the resonant frequency of about 3,19 W, which is quite low.

4.3 Marina tests

A similar set of preliminary experiments was conducted in Leixões marina, namely, the measurement of the channel's response, as described in the previous section, as well as the transmission of a longer bit stream. Such tests comprised distances from 15 to 50 meters, however, we found

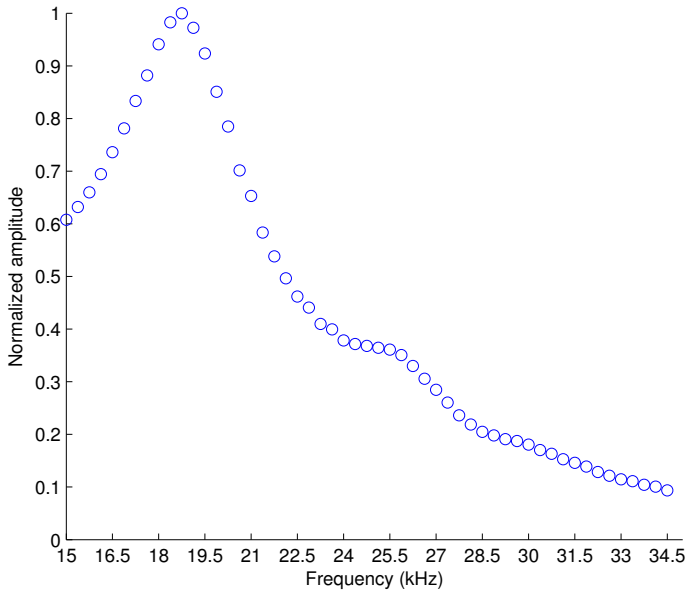

Figure 4.5: Normalized amplitude of the voltage at the transducer's terminals upon the transmission of 53 equally spaced tones in the [15;34.5] kHz band.

that above 30 meters the received signals were barely visible, probably due to the irregular objects placed along the signal's path. A representative result of the experiment regarding the channel's response is presented in Fig. 4.6, which regards an experiment where the transmitter and the receiver (the recorder) were on consecutive floating docs separated by approximately 20 meters. It is clear that this environment is much less prone to multipath than the tank as the amount of reverberation after the pulse is negligible.

In spite of this convenient property, this channel is not by any means less challenging than the tank, as was proved by a BER of 1.421×10^{-1} upon the transmission of 2048 bits at a 50 meter distance. As indicated by the bit error pattern in Fig. 4.7, the errors are approximately evenly distributed throughout the length of the signal, except for the segment [800; 1050] where they have a higher prominence. Once again, the temporal evolution of the amplitudes of the relevant DFT bins is the key to understand the origins of such high error rate. To that end, Fig. 4.8 presents the results of this analysis for two segments of the received signal: a segment pertaining to the most critical section (Fig. 4.8b) and a representative segment of the remaining parts of the signal (Fig. 4.8a). The latter indicates severe fading of the 21 kHz wave, which is clearly the main cause of errors throughout the entire time span of the signal, whereas the former suggests that in the critical section also the 25,5 kHz wave entered in a fading state, hence the complete loss of reliability. These results suggest coherence times on the order of 70 ms at 25,5 kHz and above 5 s at 21 kHz and a coherence bandwidth below 4,5 kHz since the waves fade independently.

Finally, a short comment must be addressed to the apparent disparity between BERs at the marina described herein and those reported in [3]. Firstly, our test regarded a end to end distance of 20 m whereas in the case of the previous work this distance was only 5 m. Secondly, and most

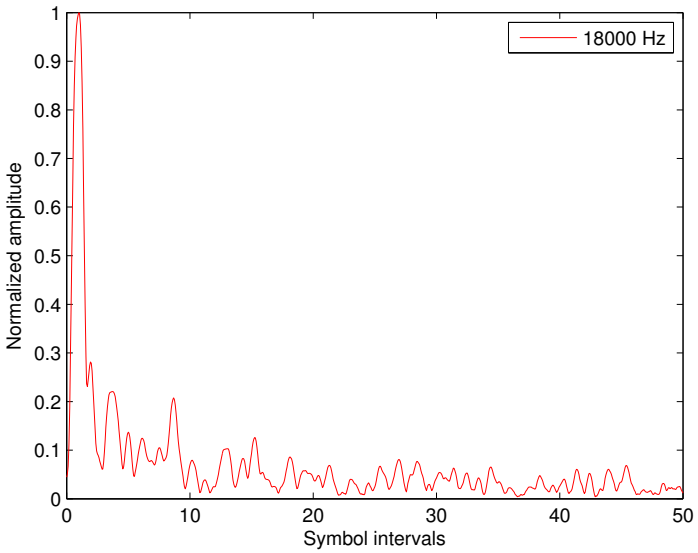

Figure 4.6: Normalized absolute value of the 18 kHz DFT bin along time upon the transmission of single symbol in that frequency at the marina. Relevant parameters: 20 m distance, 750 symbols/s baud rate, 256 point DFT, an overlapp factor of 15/16 and 240 out of 255 transmission gain.

importantly, the main cause of errors in this environment is highly time- and frequency-dependent, as was demonstrated throughout this section. Therefore, BERs of lowest orders are also achievable although such results are not as representative of the very nature of the channel as those reported herein.

4.4 Conclusion

The discussion in this chapter as well as the bit error pattern presented in Sec. 3.2 provided an insight into three different and yet quite representative channels: a multipath contaminated and highly static channel (the tank), a time varying channel very prone to fading (the marina) and a clear channel with severe motion induced Doppler (the off-coast environment). The discussion presented hereinafter will regard the conclusions derived from this study as the main goal of this dissertation is to develop a system able to operate reliably in very different environments such as these.

Figure 4.7: Bit error pattern upon the transmission of 2048 bits at the marina. Relevant parameters: two tones, 20 m distance, 375 symbols/s baud rate, 256 point DFT, an overlapp factor of 15/16 and 240 out of 255 transmission gain.

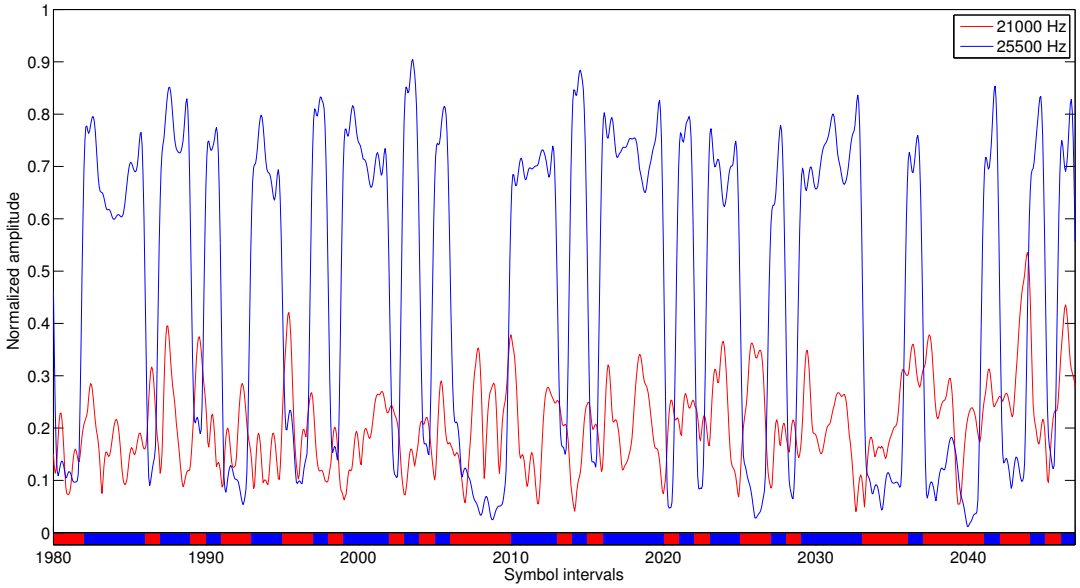

(a)

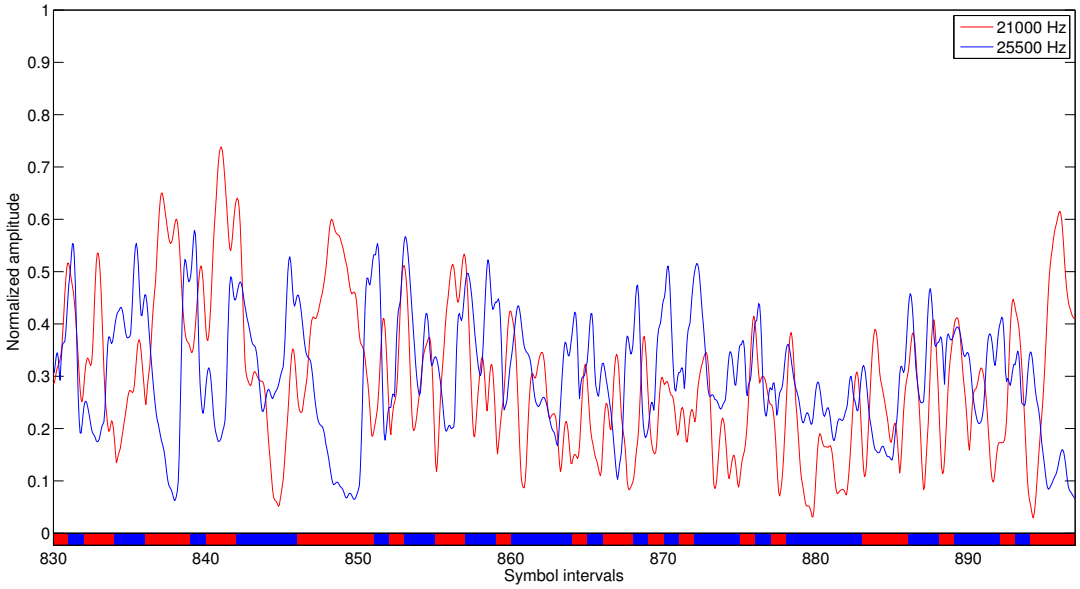

(b)

Figure 4.8: Normalized amplitude of the DFT bins of interest of two segments of received signal upon the transmission of 2048 bits at the marina: (a) Bits [1980; 2045]; (b) Bits [830; 895]. Relevant parameters: 2 tones, 20 m distance, 375 symbols/s baud rate, 256 point DFT, an overlapp factor of 15/16 and 240 out of 255 transmission gain.

Chapter 5

Enhancement Stratagies

From the discussion presented throughout the previous chapter one can conclude on the main issues that should be directly addressed through further developments: ISI caused by multipath, periodic burst errors caused by frequency selective fading and loss of synchronization due to motion induced Doppler. To that end, this chapter starts with the selection of the set of the most appropriate strategies to address such issues and increase the overall performance of the system followed by a thorough description of their development and implementation.

5.1 Design decisions

5.1.1 Strategies to overcome the encountered issues

ISI

Several techniques to overcome multipath induced ISI have been presented in Ch. 2. Probably the most effective one is adaptive equalization (e.g. decision-feedback equalization), as it actively mitigates this issue, rather than avoiding it. Even so, as stated in [19], the lack of an accurate phase estimation compromises the equalizer's performance, which renders this technique inappropriate for incoherent systems, as is the case. Another possibility would be the use of guard intervals [10, 23, 24], however, as mentioned before, more successful FSK systems rely on frequency hopping [11, 12, 44] in order to avoid the bit rate reduction caused by the idle periods. Therefore, the latter will be selected to overcome the ISI issue. Nevertheless, nearly all the mentioned papers report the use of this strategy with baud rates at least on order of magnitude lower than those used in [3] as they allow for a higher resilience to the ISI. As such, such possibility must be considered in the forthcoming work.

Frequency selective fading

Time varying frequency selective fading, in turn, could be avoided either by time or frequency diversity, as nearly all the mentioned incoherent systems use at least one of these techniques. The former, however, requires the temporal redundancy to span over the coherence time of the channel,

which would be difficult considering that coherence times above 5 s have been observed in the marina. Since the available hardware is clearly capable of exceeding the coherence bandwidth of the channel (the transducers have more than 10 kHz of available bandwidth), frequency diversity will be the selected technique. For the simplicity of implementation every symbol will have the same diversity factor and the corresponding tones will be added at the receiver. The decoded symbol will be the one for which this sum produces the highest value [11, 12].

Loss of synchronization

Although there are several techniques for timing tracking in Doppler channels, those regarding underwater acoustics, and more specifically, incoherent systems, usually rely on a short pulse or sequence which is periodically transmitted in order for the receiver to realign its timing information with the transmitter [11, 23, 45, 44]. In fact, the sync preamble described in Ch. 3 is a practical example of such procedure, therefore, a periodic repetition thereof could be thought of as a timing tracking solution. Even so, there are two main reasons not follow such approach. First of all, this algorithm is based upon the work in [40, 41], which aims towards satellite systems, consequently, it was developed for a medium of a completely different nature. Indeed, it strongly depends on amplitude information which is not entirely reliable due to the severe fluctuations caused by multipath (as we have seen in previous chapter). On the other hand, since the sync preamble has a duration of 8 symbol intervals (in the tested implementation), a periodic transmission thereof would result in a non-negligible reduction of the effective data rate. For these reasons, we decided discard this algorithm and to develop our own, inspired by the "short pulse" approach, which will be perform both the initial timing acquisition and the timing tracking without the need for a frequency acquisition algorithm. Unlike many of the mentioned systems, the pulses will be sent in parallel with the transmitted data for an increased efficiency. Additionally, this mechanism will allow for a simple estimation of the Doppler factor which can then be used to make the required adjustments to the ADC's sampling frequency.

5.1.2 Additional structural modifications

Besides the development and implementation of the mentioned strategies to overcome specific issues, an additional set of features and structural modifications will be introduced for a general enhancement of the system's performance.

Equalization at the transmitter

The experiments described in Sec. 4.2.2 proved the importance of an approximately equal power of each transmitted frequency. Since the system revealed such an unbalanced frequency response, equalization at the transmitter is required if a reliable communication is to be achieved. Furthermore, as will be explained below, the synchronization algorithm also requires the transmission of tones with different powers.

Discarding the receiver-side equalization

As discussed in Ch. 2 linear equalization is not suited for fading channels. This is due to the fact that these equalizers attempt to compensate for fading frequencies, which besides being unfruitful, can result in strong noise enhancement in that band [17]. Additionally, the diversity usage (which assigns multiple tones to a single symbol) and the equalization at the transmitter contribute for a more even energy distribution among symbols.

Discarding the header[1]

Since it was decided that the receiver-side equalization as well as the initial timing acquisition and the frequency acquisition algorithms would be discarded, the header is non longer needed, thus, the transmitted packets will now consist only of the data itself[2].

Multiple tone (MT) transmission

All the strategies discussed so far have aimed towards increasing the reliability of the system, yet, none of them promises to have a positive and direct impact on effective data rate[3]. Despite the fact that throughput of the previously develop system is actually higher than those of the majority of the studied systems, if one has to resort to a reduction of the baud rates, the throughput will of course follow the same reduction. To face this issue, several FSK systems employ multiple tone transmission [10, 23, 11] due to its increased bandwidth efficiency over MFSK modulations. As such, this feature will also be added to the system.

5.2 Implementation details

5.2.1 Synchronization algorithm

In spite of the wide range of systems that use short pulses for synchronization purposes, the corresponding papers do not provide much information on the actual implementation details, thus, we developed our own algorithm based on the conclusions drawn from an analysis of several recorded signals. The basic principle can be observed in the figures presented in the last chapter, which depict the results of transmission of single symbols. It is clear that regardless of the amount of reverberation that may follow, the rising edge of the pulse always follows a "standard" behavior. Of course, it my increase its growing rate if a an echo with an opposite phase arrives in the mean time or vice-versa, nevertheless, it always possesses some distinctive properties. One of these, is the backward finite difference taken with a separation equal to the symbol length in the ST-DFT domain, which is defined as

$$\nabla X_i[k] = X_i[k] - X_{i-\frac{1}{1-O}}[k]. \tag{5.1}$$

[1] Since the header had to be manually sent, i.e. the header was actually a part of the bit stream, this decision results only in changes at the receiver.

[2] This is due to the fact that the new synchronization algorithm will operate in parallel.

[3] Of course, increasing the system's reliability allows for the use of less parity bits in the bit stream which, indeed, increases the effective information data rate.

In fact, it is clear that this measure increases upon the beginning of a new symbol in the corresponding bin, and stops increasing at the right sample instant. With this in mind, the following algorithm for the estimation of the right sample instant was developed, where k_S is the bin of the sync pulse frequency, A is a circular buffer[4] containing the highest among the last K_A values of $\nabla X_i[k]$, $\overline{A}$ is its average value, $\nabla^2 X_i[k] = \nabla X_i[k] - \nabla X_{i-1}[k]$, i is the index of the last ST-DFT computation and $\hat{t}_{S,l}$ is the estimated sample time of symbol l.

$A \leftarrow 0$
$i \leftarrow 0$

For $i = 1 : K_{ini}$
  If $\nabla X_i[k_S] > K_{thresh1}\overline{A}$
    Add $\nabla X_i[k_S]$ to A

While $\nabla X_i[k] < K_{thresh2}\overline{A}$
  If $\nabla X_i[k_S] > K_{thresh1}\overline{A}$
    Add $\nabla X_i[k_S]$ to A
  $i \leftarrow i+1$

While $\nabla^2 X_i[k_S] > K_{thresh3}\nabla^2 X_{i-1}[k_S]$
  $i \leftarrow i+1$

$\hat{t}_{S,0} \leftarrow i$

Therefore, this algorithm basically waits for a difference much higher then the usual and then estimates the right sample instant as the moment when the difference slows its increasing rate. Of course, in order for this method to work, there are two main requirements:

Sync pulses cannot be sent at the symbol rate

Since the algorithm requires the channel to be initially clear, the separation between consecutive pulses must exceed the total multipath span. Consequently, sampling between pulses must be performed through the addition of the corresponding number of symbol intervals to the last sample instant estimate, i.e. $\hat{t}_{S,l} = \hat{t}_{S,0} + l\frac{1}{1-O}, l = 0,1,...N_P$, where N_P is the number of symbols between consecutive sync pulses.

The amplitude of the pulses must be higher than that of the other tones

Naturally, during transmission the noise in the sync tone bin rises significantly due to the side lobes of the remaining tones. Since this factor compromises the performance of the algorithm, the sync tones will be transmitted with a higher power, as this allows for a lower sensitivity to the noise. Such will be accomplished through the mentioned transmitter-side equalization.

[4] This means each time an element is added to the buffer, it is written on the position of the oldest element therefore removing it from the buffer.

Diversity must also be implemented for the sync tones

Just as the tones the actually carry information, the sync tones must also be protected with diversity, otherwise, they would be prone to fading and the entire performance of the synchronization algorithm would be compromised.

Finally, a selection of the most appropriate parameters for this algorithm had to be performed. In regards to the amount of overlap of ST-DFT, high factors result in more amplitude fluctuations which give rise to misinterpretations on behalf of the algorithm, whereas low factors reduce the accuracy of the estimated instant. After some experiments, it was concluded that the overlap factor 7/8 allowed for the best trade-off in this sense. Hence, the worst-case timing error (assuming an optimum selection of the sample instant) is of 1/16 of the symbol period. As for the constants $K_{thresh1}$, $K_{thresh2}$ and $K_{thresh3}$, it was concluded that the values of 1/2, 16 and 1/2, respectively, allowed for the best average performance in all channels, while also being suited for the hardware implementation (all of them are powers of two).

5.2.2 Hardware implementation

An overview of the hardware implementation of the transmitter, before and after the mentioned structural modifications is presented in Fig. 5.1. As can be seen, the general implementation strategy consisted of replicating the DDS modules according to the number of tones that are simultaneously outputted and performing the necessary modifications to the remaining modules. The actual number is given by the combination of the maximum number of information-bearing tones (N_T), either due to diversity or to MT transmission, and the maximum number of sync tones (N_S), for diversity purposes. The modulator now simultaneously outputs each of these tones as well as each of the corresponding equalization gains, hence a number of outputs equal to $2(N_S+N_T)$. The gains are then multiplied by corresponding outputs of the DDSs, so as to perform the desired equalization at the transmitter. All the results (N_S+N_T) are accumulated before feeding the $\Sigma\Delta$ modulator.

The choice of an equalization performed by the means of gains that multiply for each sine wave instead of one relying on a FIR filter was due to the more precise and easily reconfigure nature of the former. The gains have a 6-bit width which is a well positioned in the trade-off between the resulting implementation area and resolution of the equalizer's response.

The parameters N_T and N_S are defined defined upon the synthesis of the circuit, and thus control the number of blocks that are actually generated. Although this already favors the desired flexibility of the design, the latter is even further enhanced as this values only define the maximums. This means that although the maximum number of information-bearing tones and sync tones are defined upon the synthesis of the circuit, the actual numbers, n_T and n_S[5], are real-time reconfigurable powers of two in the intervals $[1; N_T]$ and $[1; N_S]$, respectively.

[5] We chose a lower case notation to emphasize the fact that these parameters are not constant but rather real-time configurable. Such notation will be followed hereinafter.

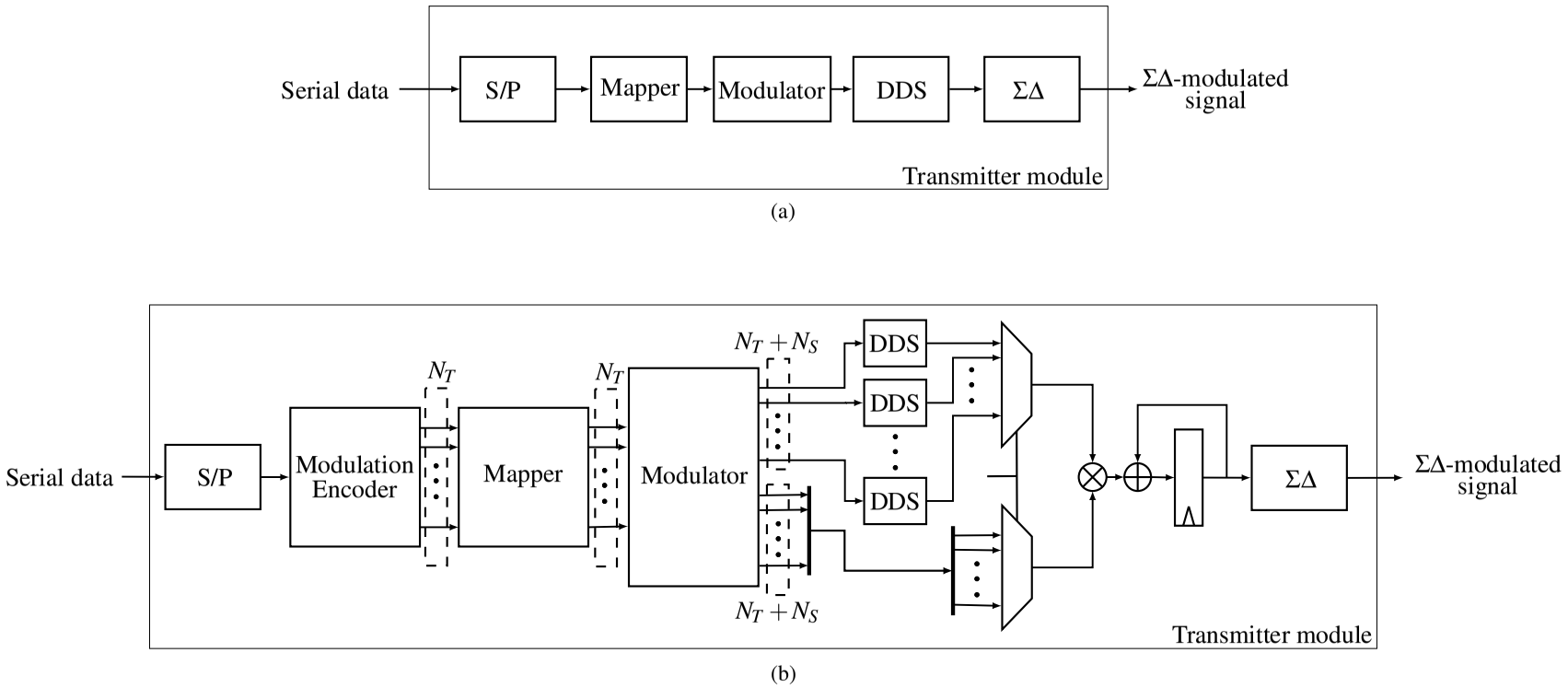

Figure 5.1: Overview of the hardware implementation of the transmitter: (a) as in [3]; (b) after the mentioned structural modifications (the encoder module has been removed as it was not implemented).

The list of major changes at the module level starts by the modulation encoder module. It basically assigns the correct symbol among those outputted in series by the S/P module to each of its N_T output streams[6] according to the the current value of n_T. For instance, if $N_T = 8$ and $n_T = 1$, this modules assigns each symbol to all output streams, as if only one symbol was being transmitted; for the same value of N_T, if $n_T = 2$, instead, it will assign one symbol to the half of the output streams and the following one to the other half, therefore doubling the output rate. As such, for a fixed value of N_T, the real-time configurable variable n_T implicitly controls the number of diversity channels para symbol and the number of independent channels (MT transmission). The mapper, which follows the described module, works just as described in Ch. 3, although it now outputs N_T symbols simultaneously.

As for the modulator implementation, major changes were performed. It has now 4 real-time configurable lookup tables, implemented as RAMs: a table with the phase increments of all the frequencies that might be transmitted, a table with the equalization gains of those frequencies, a table assigning each symbol of each output stream and hopping band to the corresponding frequency and gain (an index of the former tables) and a similar table for the sync tone frequencies. The fact that these tables are real-time reconfigurable together with the mentioned capabilities of the modulation encoder are the main reasons why one can send a number of tones lower than N_T, or equivalently, use any diversity factor lower than this value. In fact, such is accomplished by configuring the N_T output streams to the corresponding frequencies and choosing an appropriate value of n_T. For instance, if $N_T = 4$, one can choose to send only one tone simultaneously by assigning n_T to 1 and configuring all output streams to the same frequency, or one can choose to use 4 diversity channels by configuring each of the output streams to a different frequency.

This module also controls the hopping pattern as well as the timing of the sync tone transmission and both were implemented with the mentioned design philosophy: the maximum values of all parameters are constants fixed at the time of the synthesis, as they control the very nature of the modules, but the parameters that are de facto used are real-time configurable (with values at most equal to the corresponding maximums). This applies to the number of hop channels, the number of symbols between hops, and the number of symbols between consecutive sync tones.

Finally, the widths of DDSs' output and internal accumulator were kept at 14 and 20 bit, respectively, but its clock rate was lowered by a factor of 128 so as to keep the input of $\Sigma\Delta$ module constant for this number of clock cycles (a requirement thereof). As such, their frequency resolution is now 93,75/128 Hz.

[6] From now on, we will refer to each of the N_T streams that start at the modulation encoder and are finally joined by the upper multiplexer as output streams.

Chapter 6

Results

Once all the mentioned modifications were implemented, their impact was assessed through a new series of experiments similar to those described in Ch. 4. As previously mentioned, it was not possible to carry out an hardware implementation of the receiver during the time span of this dissertation. Therefore, all the tests presented this chapter consisted, once again, of the data transmission using the actual developed hardware followed a by MATLAB decoding of the recorded sounds, i.e. we followed the methodology described in Sec. 4.1.

6.1 Synthesis parameters and implementation costs

The system was synthesized with a set of fixed parameters aiming towards the adaptability to a wide range of applications. Table 6.1 shows the most relevant, mainly regarding the maximum possible values of different reconfigurable parameters.

Parameter	**Value**
Maximum number of simultaneous information-bearing tones (N_T)	8
Maximum number of simultaneous sync tones (N_S)	2
Maximum number of hop channels (N_{HC})	8
Number of entries in the modulator's frequency and gain table s	64

Table 6.1: Relevant parameters defined upon the synthesis of the modem.

The synthesis results are shown in Table 6.1, even if resource optimization was not a priority in our developments. Besides of the number of RAMs, which increased considerably due to the mentioned tables of the modulator, the usages of the other resources suffered relatively modest changes considering the nature of the implemented features. It must also be pointed out that the Xilinx Spartan-3E FPGA has rather few resources when compared to most FPGAs.

Resource	Used in [3] (%)	Used after the modifications to the system (%)
Slice Flip Flops	2664 (28%)	4402 (47%)
4 input LUTs	3428 (36%)	4915 (52%)
RAMs	8 (40%)	20 (100%)
Multipliers	4 (20%)	5 (25%)

Table 6.2: Resource usage before and after the modifications to the system.

6.2 Tests

6.2.1 Oceansys tank

From the first series of experiments in the faculty's tank (Sec. 4.2), it was clear that the main issue to be addressed in this environment was the heavy multipath structure. As was concluded in the last chapter, frequency hopping was probably the most effective feature to reduce the resulting BER, thus, its parameters had to be carefully selected. Since those experiments indicated that for a fine-tuned gain the amplitude of the reverberation would fall to half of that of the first peak after about 5 symbol intervals, tests with a number of hopping channels around the this value were conducted. We concluded that the number of hopping channels above which the BER variations became negligible was 4. On the other hand, there was no clear reason for more than one symbol to be sent simultaneously.

The parameters used in such experiments are summarized in tables 6.3 and 6.4. Table 6.5, in turn, presents some representative results in terms of BERs.

Parameter	Value
Number of independent information channels	1
Diversity factor of each information channel	1
Diversity factor of the sync channel	2
Number of symbols between sync pulses	32
Number of hopping channels	4
Number of symbols between hops	1

Table 6.3: Relevant parameters selected for the faculty's tank experiments.

These results represent a BER decrease of 3 and X orders of magnitude for the baud rates of 750 and 375 symbols per second, respectively. Fig. 6.1, where the spectrogram of a section of the recorded signal is depicted, shows how hopping allows for the reverberation to fade away before each channel is used once again. This proves that, as stated by several papers presented in Ch. 2, frequency hopping is indeed a powerful feature for coping with the ISI generated by multipath.

6.2.2 Marina

In the marina, communication could clearly benefit from diversity usage, therefore, experiments with several parameter combinations which always included some form of diversity where con-

Diversity band	Hopping channel	Symbol	Frequency (kHz)
1	1	1	18
		2	19,5
	2	1	21
		2	22,5
	3	1	24
		2	25,5
	4	1	27
		2	28,5

Table 6.4: Frequency map used in the faculty's tank experiments.

ducted. Tables 6.6 and 6.7 present those which produced the best results for the baud rate of 750 symbols and the configuration used in Sec. 4.3: the transmitter and the receiver on consecutive floating docs separated by approximately 20 meters.

In fact, we found hopping with just two channels in conjunction with two diversity channels to be the best combination for this particular situation, as this scheme not only protected the signal to fading but it provided some multipath resilience. Of course, as was demonstrated in Ch. 4, the prominence of the latter was much lower in the marina than it was in the pool, hence the choice for only two hopping channels. Among different experiments, we reached an average BER around 6×10^{-3}, which is once again two orders of magnitude lower than that of the experiments with no hopping nor diversity usage.

In spite of this interesting result, an assessment of the benefits of higher diversity factors as well as those of a higher number of independent channels was not carried out, as our transmission attempts with such schemes were either completely invisible at the receiver or resulted in highly noisy signals. In fact, as was explained in the previous chapter, the power is divided among the transmitted tones, therefore, the SNR at each individual frequency decreases with the number of tones transmitted. Of course, such lack of power is also due to the frequency response of the combination of transducer and the output circuit. Indeed, besides the high attenuation even at the resonant frequency (mainly due to the audio amplifier), this response is quite unbalanced, which results further attenuation in the equalization process.

6.2.3 Synchronization algorithm

The synchronization algorithm was used in all the experiments discussed in this chapter, and considering the results, it proved to be capable of performing the required timing acquisition and tracking. Even so, it was not tested in the presence of true motion-induced Doppler.

Unfortunately, the off-coast experiments were corrupted due to a combination of the mentioned lack of power and the high noise level generated by several boats located throughout the test scenario. Although this channel is most certainly free of both multipath and fading, and thus would not be as challenging as the those studied so far, it would an appropriate scenario for testing the algorithm's resilience to motion-induced Doppler. Since we were not able to repeat those tests

Baud rate	**BER**
750	$4,88 \times 10^{-4}$
375	$4,6 \times 10^{-3}$

Table 6.5: BERs obtained in upon the transmission of 2048 bits in the faculty's tank.

7

in the time span of this dissertation, we used a quite reliable simulation of this effect: resampling the received signal by a factor of $(1+a)$ where a (the Doppler factor) was the ratio between the simulated speed and the speed of sound. Fig. 6.2 presents the results for a text sequence with a baud-rate of 375 symbols per second with an initial error probability of $1,17 \times 10^{-2}$ and a simulation end-to-end motion of 3 meters per second.

As it can be seen in Fig. 6.2a, the sequence was decoded with a relatively low number of errors, but when a motion of 3 m/s is simulated (Fig. 6.2b), synchronization is lost after about 50 symbols, and an error pattern quite similar to that of Fig 3.4 is obtained, hence proving how accurately of this procedure simulates motion-induced Doppler. However, if the synchronization algorithm is turned on[1], the Doppler effect is virtually removed, leaving only behind a negligible in increase in the error probability, which is now $1,66 \times 10^{-2}$. This proves the algorithm is indeed capable of correcting for Doppler induced by an end-to-end speed as high as 3 m/s. It should be noted, however, that this correction is only being performed at the symbol timing level, i.e. no resampling of the signal is being performed, as will be done by the actual hardware implementation of the receiver. The possibility of using only this type of correction is due to the proximity between the frequencies we used, which is at least 750 Hz, as such values of end-to-end motion only produce a frequency deviation on the order of 200 Hz.

[1]This means, besides doing the initial timing acquisition, it also performs the timing tracking.

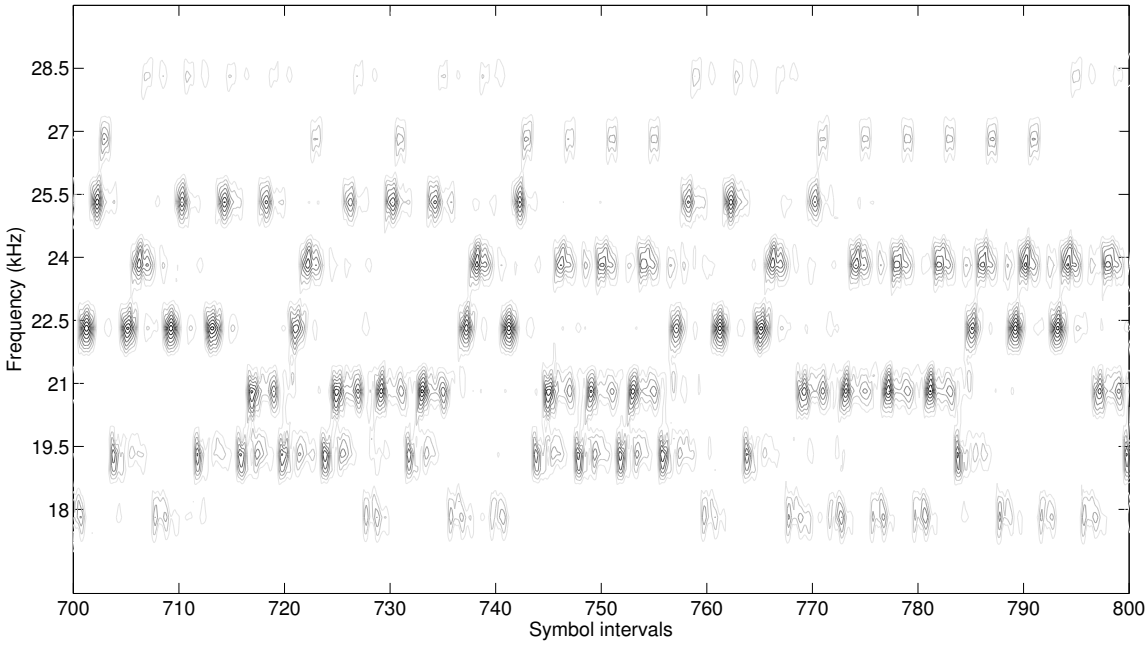

Figure 6.1: Contour plot of the spectrogram showing the hopping pattern upon the transmission of 2048 bits at the faculty's tank. Relevant parameters: 375 symbols/s baud rate, 256 point DFT, an overlap factor of 7/8 and 14 out of 255 transmission gain.

Parameter	**Value**
Number of independent information channels	1
Diversity factor of each information channel	2
Diversity factor of the sync channel	2
Number of symbols between sync pulses	32
Number of hopping channels	2
Number of symbols between hops	1

Table 6.6: Relevant parameters selected for the faculty's tank experiments.

Diversity band	**Hopping channel**	**Symbol**	**Frequency (kHz)**
1	1	1	21
		2	24
	2	1	16,5
		2	19,5
2	1	1	28,5
		2	30
	2	1	25,5
		2	27

Table 6.7: Frequency map used in the marina experiments.

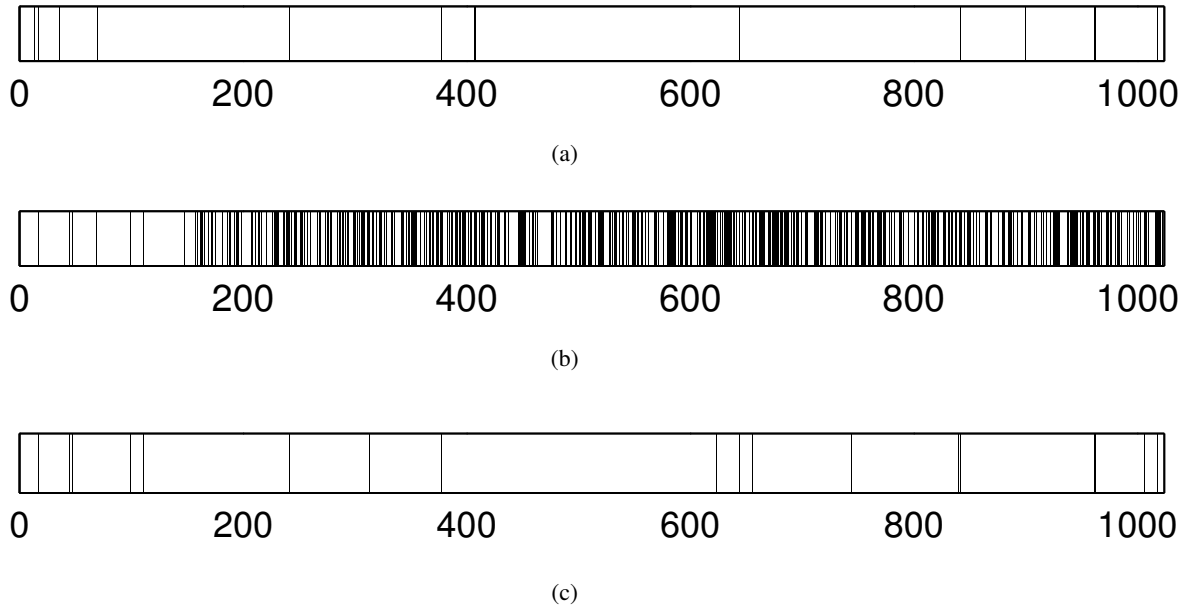

Figure 6.2: Bit error patterns of decoded sequences in the motion-induced Doppler test: (a) original decoded sequence with no motion-induced Doppler; (b) decoded sequence with a simulated end-to-end motion of 3 m/s and the sync algorithm turned off; (c) decoded sequence with a simulated end-to-end motion of 3 m/s and the sync algorithm turned on.

Chapter 7

Conclusions

In this dissertation, through a careful analysis of a previously developed system, we were able to identify the most critical aspects of its performance and use such understanding together with knowledge acquired thorough a study of the state-of-the-art in underwater acoustic communications to develop an appropriate set of solutions. More specifically, besides several minor modifications, we implemented frequency hopping, diversity usage and developed a novel algorithm timing acquisition and tracking, all of a highly reconfigurable nature. The combination of these features allowed for a two orders of magnitude reduction of the the error probability in two challenging environments and provided the system with a considerable resilience to Doppler induced by speeds quite difficult to reach when the nodes are simply drifting. Furthermore, these results proved the validity of the analysis carried out in Ch. 4 and Ch. 5. Even so, as the number of experiments was somewhat low, further tests are required to reach an appropriate assessment of the benefits of each of these features, specially for the cases of diversity usage and MT transmission. Furthermore, neither of the implemented features is obviously optimized, i.e. each feature lacks some minor refinements that would only be permitted by a more the consistent set of tests.

Unfortunately, the receiver implementation was not carried out, hence, it was not possible to obtain results regarding the actual hardware implementation. However, we believe that, due to the fidelity of the receiver replica developed in the MATLAB environment, the conclusions drawn in this dissertation will be largely transposed to the hardware implementation.

As for suggestions for future developments, among new ideas and more important requirements, we can name:

Conduction of new tests

As mentioned before, it is important to better assess the benefits of the implementation features, and perform the required adjustments. More specifically, experiment with higher diversity schemes and MT transmission in order to reach effective bit rates of 1500 bits/s or higher.

Complete implementation of the receiver modifications

This is an obvious requirement for future developments, however, it will most likely be

straightforward considering the small amount of changes and the modules that will be removed.

Incorporate the diversity and MT transmission features

Coded modulation techniques[16] and more complex selections of schemes can be easily implemented as extensions of the diversity and MT transmission features will certainly have an important impact not only in the system's robustness but mostly the effective data rate.

Implement an automatic tuning procedure of the system's parameters

In fact, if the some form of feedback on behalf of the receiver was available, the transmitter could automatically optimize the transmission parameters for each operation scenario. This idea would, of course, require more research on its feasibility and on appropriate algorithms for this purpose, as well as the implementation of a communication protocol.

References

[1] M. Stojanovic, J. Catipovic, and J. G. Proakis. Adaptive multichannel combining and equalization for underwater acoustic communications. *The Journal of the Acoustical Society of America*, 94(3):1621, 1993. URL: http://link.aip.org/link/JASMAN/v94/i3/p1621/s1&Agg=doi, doi:10.1121/1.408135.

[2] D.B. B Kilfoyle and A.B. B Baggeroer. The state of the art in underwater acoustic telemetry. *IEEE Journal of Oceanic Engineering*, 25(1):4–27, January 2000. URL: http://ieeexplore.ieee.org/xpls/abs_all.jsp?arnumber=820733http://ieeexplore.ieee.org/lpdocs/epic03/wrapper.htm?arnumber=820733, doi:10.1109/48.820733.

[3] Henrique Cabral. Acoustic modem for underwater communication. Master's thesis, Faculdade de Engenharia da Universidade do Porto, 2014.

[4] Milica Stojanovic. Underwater Acoustic Communications: Design Considerations on the Physical Layer. *Fifth Annual Conference on Wireless on Demand Network Systems and Services*, (2), January 2008. URL: http://ieeexplore.ieee.org/lpdocs/epic03/wrapper.htm?arnumber=4459349, doi:10.1109/WONS.2008.4459349.

[5] R J Urick. *Principles of underwater sound*. McGraw-HiII, New York, 1983.

[6] Finn B. Jensen, William A. Kuperman, Michael B. Porter, and Henrik Schmidt. *Computational Ocean Acoustics*. Springer, New York, NY, 2011. URL: http://link.springer.com/10.1007/978-1-4419-8678-8, doi:10.1007/978-1-4419-8678-8.

[7] R. Price and P. Green. A Communication Technique for Multipath Channels. *Proceedings of the IRE*, 46(3):555–570, March 1958. URL: http://ieeexplore.ieee.org/lpdocs/epic03/wrapper.htm?arnumber=4065360, doi:10.1109/JRPROC.1958.286870.

[8] J.G. Proakis. *Digital Communications*. McGraw-Hill Series in Electrical and Computer Engineering. Computer Engineering. McGraw-Hill, 2001. URL: http://books.google.pt/books?id=sbr8QwAACAAJ.

[9] Milica Stojanovic. Recent advances in high-speed underwater acoustic communications. *IEEE Journal of Oceanic Engineering*, 21(2):125–136, April 1996. URL: http://ieeexplore.ieee.org/lpdocs/epic03/wrapper.htm?arnumber=486787, doi:10.1109/48.486787.

[10] S. Morgera. Multiple terminal acoustic communications system design. *IEEE Journal of Oceanic Engineering*, 5(3):199–204, July 1980. URL: http://ieeexplore.ieee.org/lpdocs/epic03/wrapper.htm?arnumber=1145465, doi:10.1109/JOE.1980.1145465.

[11] J. Catipovic, A. Baggeroer, K. Von Der Heydt, and D. Koelsch. Design and performance analysis of a Digital Acoustic Telemetry System for the short range underwater channel. *IEEE Journal of Oceanic Engineering*, 9(4):242–252, October 1984. URL: http://ieeexplore.ieee.org/lpdocs/epic03/wrapper.htm?arnumber=1145632, doi:10.1109/JOE.1984.1145632.

[12] K.F. Scussel, J.A. Rice, and S. Merriam. A new mfsk acoustic modem for operation in adverse underwater channels. In *OCEANS '97. MTS/IEEE Conference Proceedings*, volume 1, pages 247–254 vol.1, Oct 1997. doi:10.1109/OCEANS.1997.634370.

[13] J. Catipovic, M. Deffenbaugh, L. Freitag, and D. Frye. An Acoustic Telemetry System for Deep Ocean Mooring Data Acquisition and Control. In *Proceedings OCEANS '89*, volume 3, pages 887–892, Seattle, WA, USA, 1989. IEEE. URL: http://ieeexplore.ieee.org/lpdocs/epic03/wrapper.htm?arnumber=586702, doi:10.1109/OCEANS.1989.586702.

[14] Mandar Chitre, Shiraz Shahabudeen, and Milica Stojanovic. Underwater Acoustic Communications and Networking: Recent Advances and Future Challenges. *Marine Technology Society Journal*, 42(1):103–116, March 2008. URL: http://openurl.ingenta.com/content/xref?genre=article&issn=0025-3324&volume=42&issue=1&spage=103, doi:10.4031/002533208786861263.

[15] M. Badiey, J. Simmen, and S. Forsythe. Frequency dependence of broadband propagation in coastal regions. *The Journal of the Acoustical Society of America*, 101(6), 1997.

[16] J.G. Proakis. Coded modulation for digital communications over Rayleigh fading channels. *IEEE Journal of Oceanic Engineering*, 16(1):66–73, 1991. URL: http://ieeexplore.ieee.org/lpdocs/epic03/wrapper.htm?arnumber=64886, doi:10.1109/48.64886.

[17] J.G. Proakis. Adaptive equalization techniques for acoustic telemetry channels. *IEEE Journal of Oceanic Engineering*, 16(1):21–31, 1991. URL: http://ieeexplore.ieee.org/lpdocs/epic03/wrapper.htm?arnumber=64882, doi:10.1109/48.64882.

[18] M. Stojanovic, J.A. Catipovic, and J.G. Proakis. Phase-coherent digital communications for underwater acoustic channels. *IEEE Journal of Oceanic Engineering*, 19(1):100–111, 1994. URL: http://ieeexplore.ieee.org/lpdocs/epic03/wrapper.htm?arnumber=289455, doi:10.1109/48.289455.

[19] D.D. Falconer. Jointly adaptive equalization and carrier recovery in two-dimensional digital communication systems. *Bell System Technical Journal, The*, 55(3):317–334, March 1976. doi:10.1002/j.1538-7305.1976.tb03317.x.

[20] Trym H. Eggen. Underwater Acoustic Communication Over Doppler Spread Channels. PhD thesis, Massachusetts Institute of Technology and Woods Hole Oceanographic Institute, 1997.

[21] B.S. Sharif, J Neasham, O.R. Hinton, and A.E. Adams. A computationally efficient Doppler compensation system for underwater acoustic communications. *IEEE Journal of Oceanic Engineering*, 25(1):52–61, January 2000. URL: http://ieeexplore.ieee.org/lpdocs/epic03/wrapper.htm?arnumber=820736, doi:10.1109/48.820736.

[22] P. Qarabaqi and M. Stojanovic. Statistical characterization and computationally efficient modeling of a class of underwater acoustic communication channels. *Oceanic Engineering, IEEE Journal of*, 38(4):701–717, Oct 2013. doi:10.1109/JOE.2013.2278787.

[23] D. Wax. MFSK–The Basis for Robust Acoustical Communications. In *OCEANS 81*, pages 61–66. IEEE, 1981. URL: http://ieeexplore.ieee.org/lpdocs/epic03/wrapper.htm?arnumber=1151680, doi:10.1109/OCEANS.1981.1151680.

[24] D. Garrood and N. Miller. Acoustic telemetry for underwater control. In *OCEANS 82*, pages 111–114, Sept 1982. doi:10.1109/OCEANS.1982.1151741.

[25] G.E. Atkin and H.P. Corrales. An efficient modulation/coding scheme for MFSK systems on bandwidth constrained channels. *IEEE Journal on Selected Areas in Communications*, 7(9):1396–1401, 1989. URL: http://ieeexplore.ieee.org/lpdocs/epic03/wrapper.htm?arnumber=44578, doi:10.1109/49.44578.

[26] G. Mackelburg, S. Watson, and A. Gordon. Benthic 4800 BITS/S Acoustic Telemetry. In *OCEANS 81*, pages 72–72. IEEE, 1981. URL: http://ieeexplore.ieee.org/lpdocs/epic03/wrapper.htm?arnumber=1151696, doi:10.1109/OCEANS.1981.1151696.

[27] Milica Stojanovic. Low Complexity OFDM Detector for Underwater Acoustic Channels. In *OCEANS '06*, Boston, MA, USA, September 2006. IEEE. URL: http://ieeexplore.ieee.org/lpdocs/epic03/wrapper.htm?arnumber=4098876, doi:10.1109/OCEANS.2006.307057.

[28] Ross E. Williams and Henry F. Battestin. Coherent Recombination of Acoustic Multipath Signals Propagated in the Deep Ocean. *The Journal of the Acoustical Society of America*, 50(6A), 1971. URL: http://link.aip.org/link/JASMAN/v50/i6A/p1433/s1&Agg=doi, doi:10.1121/1.1912785.

[29] Neptune Sonar. *T257 Datasheet*.

[30] Nuno A. Cruz. *Emissão de Sinais Acústicos Subaquáticos*, 2007.

[31] Helder S Campos and José C Alves. Reconfigurable Signal Processing Platform for Underwater Localization. In *Proceedings of the XVIII Conference on the Design of Circuits and Integrated Systems*, pages 164–169, San Sebastian, Spain, 2013.

[32] STMicroelectronics. 10W Car Radio Audio Amplifier, 1998. TDA2003 datasheet.

[33] Michael Randelzhofer. *GODIL User Manual*. OHO-Elektronik, Dachau, Germany, v 0.91 edition, 2009. URL: http://www.oho-elektronik.de/pics/UM_GODIL.pdf.

[34] Xilinx Inc. Spartan-3E FPGA Family Data Sheet, 2013.

[35] Xilinx Inc. *PicoBlaze 8-bit Embedded Microcontroller User Guide*, 2011. URL: http://www.xilinx.com/support/documentation/ip_documentation/ug129.pdf.

[36] Xilinx Inc. LogiCORE IP DDS Compiler v4.0, 2011. URL: http://www.xilinx.com/support/documentation/ip_documentation/dds_ds558.pdf.

[37] Xilinx Inc. IP LogiCORE FIR Compiler v5.0, 2011. URL: http://www.xilinx.com/support/documentation/ip_documentation/fir_compiler_ds534.pdf.

[38] Alan V. Oppenheim, Ronald W. Schafer, and John R. Buck. *Discrete-time Signal Processing*. Prentice-Hall, Inc., Upper Saddle River, NJ, USA, 2nd edition, 1999.

[39] Richard G. Lyons. *Understanding Digital Signal Processing*. Addison-Wesley Longman Publishing Co., Inc., Boston, MA, USA, 1st edition, 1996.

[40] S. Hara, A. Wannasarnmaytha, Y. Tsuchida, and N. Morinaga. A novel FSK demodulation method using short-time DFT analysis for LEO satellite communication systems. *IEEE Transactions on Vehicular Technology*, 46(3):625–633, 1997. URL: http://ieeexplore.ieee.org/lpdocs/epic03/wrapper.htm?arnumber=618188, doi:10.1109/25.618188.

[41] E. Grayver and B. Daneshrad. A low-power all-digital FSK receiver for space applications. *IEEE Transactions on Communications*, 49(5):911–921, May 2001. URL: http://ieeexplore.ieee.org/lpdocs/epic03/wrapper.htm?arnumber=923814, doi:10.1109/26.923814.

[42] MarSensing Lda. *digitalHyd SR-1 Datasheet*.

[43] J Allen. Short-term spectral analysis, and modification by discrete fourier transform. *IEEE Transactions on Acoustics Speech and Signal Processing*, 25(3):235–238, 1977.

[44] M.D. Green and J.a. Rice. Channel-tolerant FH-MFSK acoustic signaling for undersea communications and networks. *IEEE Journal of Oceanic Engineering*, 25(1):28–39, January 2000. URL: http://ieeexplore.ieee.org/lpdocs/epic03/wrapper.htm?arnumber=820734, doi:10.1109/48.820734.

[45] T.H. Eggen, a.B. Baggeroer, and J.C. Preisig. Communication over Doppler spread channels. Part I: Channel and receiver presentation. *IEEE Journal of Oceanic Engineering*, 25(1):62–71, January 2000. URL: http://ieeexplore.ieee.org/lpdocs/epic03/wrapper.htm?arnumber=820737, doi:10.1109/48.820737.